Äspö Hard Rock Laboratory

Prototype Repository

Acoustic emission and ultrasonic monitoring results from deposition hole DA3545G01 in the Prototype Repository between October 2005 and March 2006

J.R. Haycox
W.S. Pettitt

Applied Seismology Consultants

August 2006

SKB

Äspö Hard Rock
Laboratory

Äspö Hard Rock Laboratory

Prototype Repository

Acoustic emission and ultrasonic monitoring results from deposition hole DA3545G01 in the Prototype Repository between October 2005 and March 2006

J.R. Haycox

W.S. Pettitt

Applied Seismology Consultants

August 2006

Report DLV-06-02

To

SKB

APPLIED SEISMOLOGY CONSULTANTS

Last Edited	7 November 2006
File name	SKB ProtoHeating to Mar06_25082006.doc
Last Printed	7 November 2006
Signature	

Executive summary

This report describes results from acoustic emission (AE) and ultrasonic monitoring around a canister deposition hole (DA3545G01) in the Prototype Repository Experiment at SKB's Hard Rock Laboratory (HRL), Sweden. The experiment has been designed to simulate a disposal tunnel in a real deep repository for disposal of high-level radioactive waste.

The monitoring aims to examine changes in the rock mass caused by an experimental repository environment, in particular due to thermal stresses induced from canister heating and pore pressures induced from tunnel sealing. Two techniques are utilised here to investigate the processes occurring within the rock mass around the deposition hole. AE monitoring is a 'passive' technique similar to earthquake monitoring but on a much smaller distance scale (source dimensions of millimetres). AEs occur on fractures in the rock when they are created or when they move. Ultrasonic surveys are also used to 'actively' examine the rock. In this case an array of transmitters sends signals to an array of receivers. Amplitude and velocity changes on the ray paths have then be used to examine changes in the rock's properties (Young's modulus, Poisson's ratio, Crack density and Saturation).
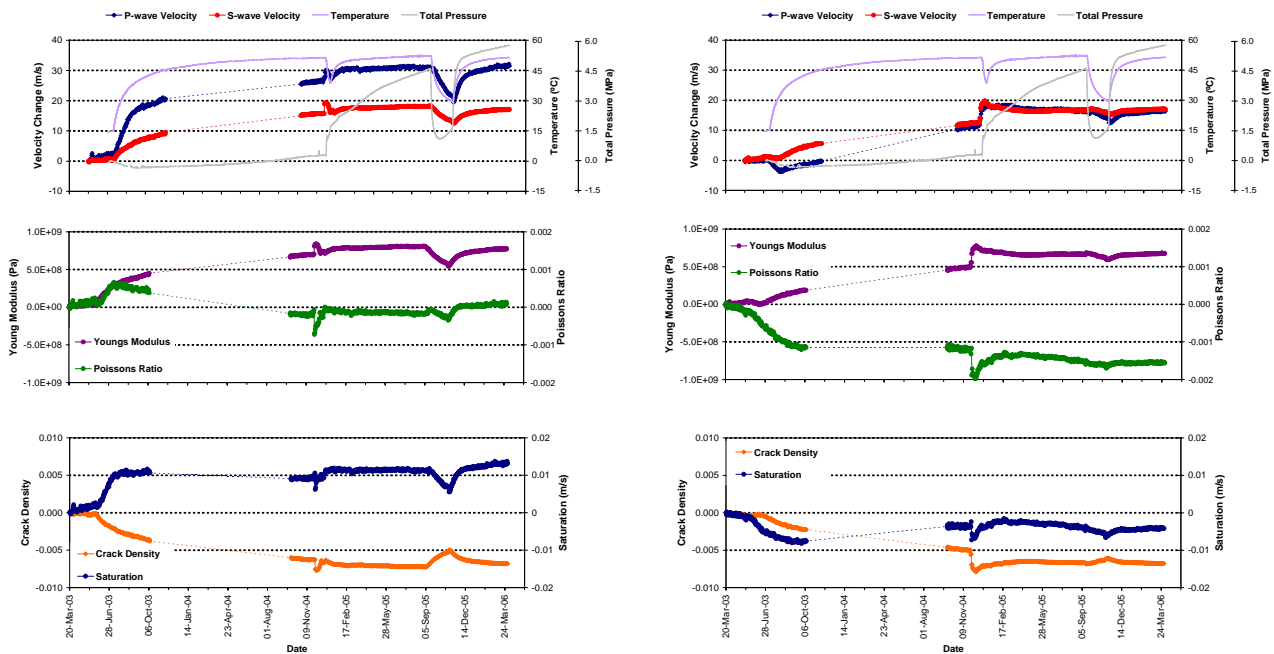
This monitoring period relates to six-months between 1st October 2005 and 31st March 2006. Since September 2005, temperature around the deposition hole is observed to decrease. On 3rd November 2005, the temperature is observed to increase after heaters are switched on again. Pressure is observed to increase from 1st November 2005. Pressure and temperature initially increase rapidly, but then steady at a constant rate of 0.1MPa and 0.9° per month respectively for the rest of the reporting period.

AE and Ultrasonic monitoring has previously been conducted at the Prototype Repository during excavation of two deposition holes in Section II of the tunnel and when simulated canisters, installed in the deposition holes, were first heated and the tunnel pressurised. Monitoring is now continuing in 6-monthly reporting periods using a permanent ultrasonic array, with transducers installed into instrumentation boreholes in June 2002, before the tunnel was sealed. In April 2003 heaters in the simulated waste canisters were switched on causing temperatures to rapidly increase in the rock mass up to approximately 50°C at the rock wall. In November 2004 water drainage from the sealed Prototype tunnel was stopped causing a rapid increase in fluid pressures in the deposition hole. An exponential decrease in temperature and pressure occurred when heaters were switched off and additional drainage to the tunnel was opened in September 2005.

Velocity changes are measured between transmitter-receiver pairs on the daily ultrasonic surveys using a cross-correlation technique that allows a velocity resolution of $\pm 2m.s^{-1}$. Average P- and S-wave velocity reduces over the first month at a consistent rate with P-wave velocity decreasing slightly faster than S-wave velocity. A variation is also observed in the average amplitude measurements during the time period. For the first month, P- and S-wave amplitudes decrease at a relatively constant rate. A minimum is reached on 6th November 2005. After this date both P- and S-wave velocities increase, such that by the end of the reporting period average velocity is slightly faster than at the start. Similarly, amplitudes rapidly increase, closely

correlating with temperature and pressure measured around the deposition hole. By the end of the reporting period, the P and S-wave amplitudes are slightly higher than at the start. The S-wave is shown to be slightly more responsive than P-wave.

Rock parameters (Young's Modulus, Poisson's Ratio, Crack Density and Saturation) have been calculated from the average measured velocities for the ray path categories. Young's Modulus decreases when the rock is de-pressurised and temperatures are reduced. Crack density increases during the first month of the monitoring period, when cooling and de-pressurisation led to microcracks reopening. The rock parameters have been compared between ray path positions with respect the deposition hole geometry. Least affected by the pressure and temperature variations is the 'Far' raypath category. Ray paths that skim close to the deposition hole surface in the 'S3' category show the largest reduction. These raypaths pass through a zone of tensile or low compressive stresses. Microfractures in this region are most responsive to changes in thermal stress due to being under low stress. When pressure and temperature increase, the crack density is observed to reduce, particularly on the 'S3' raypath category.

Velocity and modulus change for raypaths passing close to the deposition hole through the tensile zone (left) and the compressive zone (right).

The initial reduction in the stiffness of rock around the deposition hole, and increase in crack density, is a continuation of conditions that existed at the end of the previous monitoring period. The response is interpreted as an opening of existing microfractures and pore spaces in the region of low-compressive or tensile stresses. This is a result of a cooling of the rock and reduction in pressure from the deposition hole interior, returning the rock to a state prior to heating when microfractures were relatively more open. When temperature and pressure increase, the associated increase in stiffness and decrease in crack density can be interpreted as the closing of existing microfractures and pore spaces. Existing microcracks in the low-compressive or tensile region were initially unloaded immediately after excavation. Consequently they are more reactive to stress changes than in the compressive region where stresses act to pre-close the microcracks. Large changes were also observed on this category when heating commenced.

Fifty AEs have been located with high confidence from 100 triggered events recorded during this period. An average number of 0.27 events are located per day, with no more than 2 AEs located on a single day. This is an increase on the previous six months (0.21 event per day), but lower than six months before (0.32 events per day). The majority of the events locate in the immediate vicinity of deposition hole DA3545G01. Three events also locate close to the neighbouring deposition hole DA3551G01. A cluster of 39 events is situated on the SE side of deposition hole DA3545G01 at a depth of 455.1m in the low-compressive, or tensile, stress region. The events observed during this reporting period are consistent with these previous results with events locating in regions of previous activity. The events are therefore interpreted as a continuation of activity in the previously imaged damage zone and, similar to during excavation and initial heating, are created either by movement on pre-existing microcracks, or as a result of extension or formation of new microcracks in the existing damaged region.

The frequency of located events has generally been low compared to when temperature first increased in 2003 and when the rapid change in pressure occurred in December 2004. A low number of AEs suggests the rock mass has stabilised. Despite a rapid increase in temperature during this monitoring period, the rate of AEs is still low and consistent with previous monitoring. Pressure decreased rapidly in September 2005 when drainage to the tunnel was opened. Drainage closed again approximately 2 months later leading to a rapid increase in pressure. This appears to have no significant affect on the number, or distribution of AEs around the deposition hole. This differs to the results in December 2004 when a rapid pressure *increase* caused 32 events to locate in clusters over the course of two days. The events recorded then were interpreted as stress changes in the rock as it responds to the sudden pressure change. This induces small scale movement on pre-existing microcracks, or induces new microfractures in weaker volumes of the rock. Although a cluster of events has been located over the last 6 months, changes in pressure and temperature have not caused a sufficient redistribution of stresses to initiate further microfracturing.

Sammanfattning

I denna rapport redovisas resultat från akustisk utstrålning (AE) och ultraljudsmätning runt ett deponeringshål (DA3545G01) i Prototype Repository vid SKB:s Hard Rock Laboratory (HRL) i Sverige. Experimentet har konstruerats för att simulera en deponeringstunnel i ett verkligt djupförvar för högaktivt radioaktivt avfall.

Syftet med mätningen är att undersöka förändringar i bergmassan som orsakats av en experimentell förvarsmiljö, särskilt med avseende på värmespänning från uppvärming av kapseln och portryck från förseglingen av tunnel. Två tekniker används för att undersöka de processer som inträffar i bergmassan runt deponeringshålet. AE-övervakning är en 'passiv' teknik som liknar jordbävningsövervakning men på en mycket mindre avståndsskala (källdimensioner på millimetrar). AE (Acoustic Emission) uppkommer hos bergssprickor när de bildas eller när de rör sig. Ultraljudsmätning används också för att 'aktivt' undersöka berget. Vid denna mätning sänder en grupp av givare signaler till en grupp av mottagare. Förändringar i amplitud och hastighet hos signalen när den passerat genom bergmassan i olika signalvägar relativt deponeringshålen,´("ray path") har sedan använts för att undersöka förändringar i bergegenskaperna (elasticitetsmodul, Poissonstal, spricktäthet och mättnadsgrad).

Denna rapportering omfattar mätningar gjorda under sex månader mellan 1 oktober 2005 och 31 mars 2006. Man har observerat att temperaturen runt deponeringshålet har minskat sedan september 2005. Den 3 november 2005 noterar man att temperaturen ökar efter det att värmeelementen i kapsel 6 slagits på igen. Tryck och temperatur ökar hastigt till en början, men stabiliseras sedan vid konstant nivå på respektive 0,1 MPa och 0.9° per månad under resten av rapporteringsperioden.

AE och ultraljudsmätningar har tidigare utförts vid Prototypförvaret under borrning av två deponeringshål i Sektion II, vid den initiala uppvärmningen av kapslarna i deponeringshålen och när tunneln trycksattes (dräneringen av tunneln upphörde). Mätningarna fortsätter nu i 6-månaders rapporteringsperioder där man använder en permanent ultraljudssystem med sensorer installerade i borrhål i juni 2002 innan tunneln fylldes igen med återfyllning. I april 2003 slogs värmarna som installerats i kapslarna på, och detta gjorde att temperaturen snabbt steg i bergmassan, upp till ca 50°C vid bergväggen i deponeringshålen. I november 2004 stängdes dräneringen av prototyptunneln vilket orsakade en snabb ökning portrycket i deponeringshålet. En exponentiell minskning av temperatur och tryck inträffade när uppvärmningen stängdes av och ytterligare ett utflöde till tunneln öppnades i september 2005.

Hastighetsförändringar uppmättes mellan givare och sändare vid de dagliga ultraljudsmätnningarna med hjälp av en kors-korrelationsteknik som tillåter en hastighetsupplösning på $\pm 2 m.s^{-1}$. Genomsnittliga P- och S-vågshastigheterna minskar under den första månaden med en konstant hastighet, där P-vågshastigheten minskar aningen snabbare än S-vågshastigheten. En förändring kan också ses vid de genomsnittliga amplitudsmätningarna under tidsperioden. Under den första månaden minskar P- och S-vågsamplituderna med en relativt konstant hastighet. Minimum uppnåddes den 6 november 2005. Efter detta datum ökar både P- och S-vågshastighetern så att den genomsnittliga hastigheten vid slutet av rapportperioden är något högre än vid starten. På liknande sätt ökar amplituden i en takt som är korrelerat

till temperatur och tryck som uppmätts runt deponeringshålet. Vid slutet av rapportperioden är P- och S-vågsamplituderna något högre än vid starten. S-vågen visar sig vara något mer känslig än P-vågen.

Bergmassans egenskaper (elasticitetsmodul, Poissons tal, spricktäthet och mättnadsgrad) har beräknats från de genomsnittligt uppmätta hastigheterna för de olika kategorier av "signalvägar". Elasticitetsmodulen minskar när porttrycket i berget avtar och när temperaturerna sjunker. Spricktätheten ökar under den första månaden av mätperioden när avkylning och minskat portryck leder till att mikrosprickorna åter öppnas. Bergmassans egenskaper har jämförts mellan olika "signalvägar" läge i förhållande till deponeringshålets geometri. Minst påverkad av tryck- och temperaturvariationerna är de bortre "signalvägarna" dvs där signaler passerar genom berg en bit från deponeringshålet. "Signalvägar" som passerar nära deponeringshålets periferi (kategori 'S3') uppvisar den största minskningen. Dessa "signalvägar" passerar genom en zon med drag- eller låga tryckspänningar. Mikrosprickorna i dessa zoner är mest känsliga för förändringar i termisk spänning eftersom de är utsatta för låg spänning. När tryck och temperatur ökar visar det sig att spricktätheten minskar, särskilt för "signalvägar" av typen 'S3'.
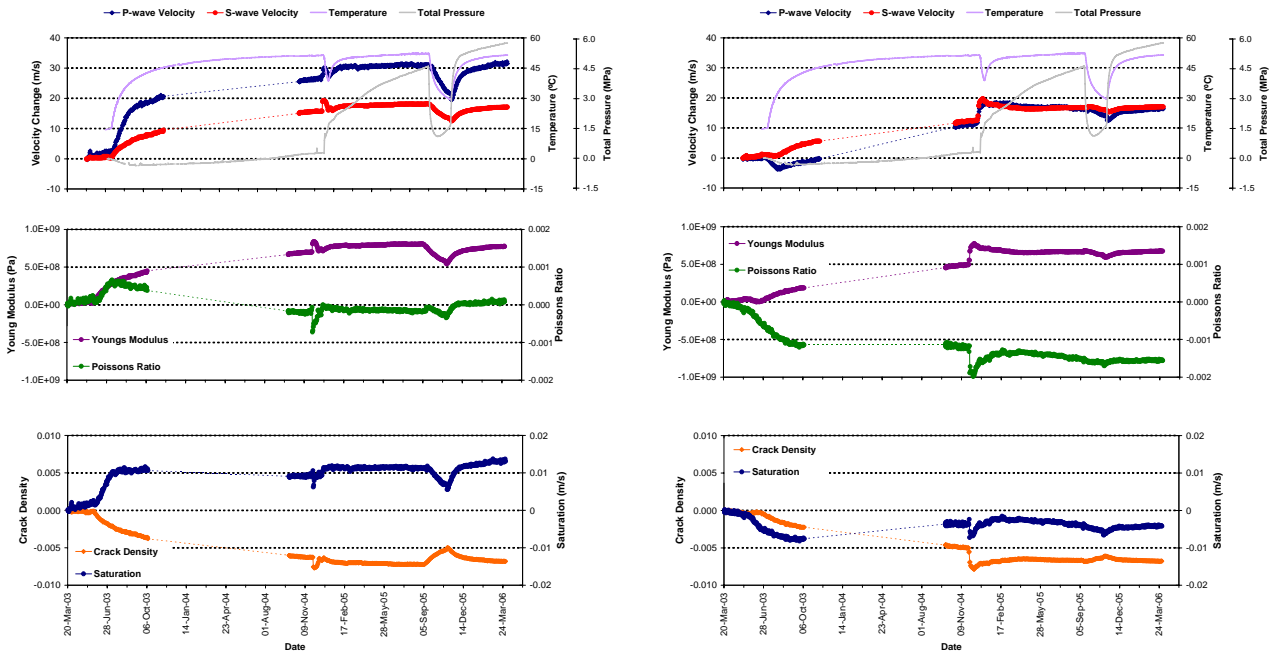
Hastighet och modulförändring för "signalvägar" som passerar nära deponeringshålet genom zonen med dragspänningar (vänster) och zonen med tryckspänningar(höger).

Den initiala minskningen av bergets styvhet runt deponeringshålet och ökningen av spricktäthet är en följd av förhållandena som rådde vid slutet av föregående mätperiod. Resultaten tolkas som en öppning av befintliga mikrosprickor och porutrymme i området med låga drag- eller tryckpåkänning inträffar. Detta är en följd av kylningen av berget och minskningen av trycket från deponeringshålets inre som gör att berget återgår till förhållandena som rådde före upphettning när mikrosprickorna var relativt sett mer öppna. När temperatur och tryck ökar kan den medföljande ökningen av styvhet och minskning av sprickdensitet tolkas som att existerande mikrosprickor och porutrymmen stängs. Existerande mikrosprickor i området med låg tryckspänningar eller dragspänningar blev till att börja med obelastade direkt efter utgrävning.

10

Följaktligen är de sprickorna mer känsliga för förändringar i spänning än i den trycksatta zonen där tryck medverkar till att stänga mikrosprickorna i förväg. Stora förändringar observerades också i denna kategori av sprickor när upphettningen påbörjades.

Femtio AE har lokaliserats med stor sannolikhet, baserat på 100 utlösta händelser som noterats under denna period. Ett antal av i medeltal 0,27 händelser har lokaliserats per dag, men inte mer än 2 AE för en enskild dag. Detta är en ökning från föregående sexmånadersperiod (0,21 händelser per dag), men en minskning jämfört med sexmånadersperioden före det (0,32 händelser per dag). Majoriteten av händelserna är lokaliserade till den absoluta närheten av deponeringshål DA3545G01. Tre händelser är lokaliserade till det närliggande deponeringshålet DA3551G01. En samling av händelser är lokaliserade till den sydöstra sidan av deponeringshål DA3545G01 på 455.1 meters djup i området med låga tryckspänningar eller dragspänningar. Händelserna som observerats under denna rapporteringsperiod är konsistenta med tidigare resultat. Händelserna tolkas därför som en fortsättning av aktivitet i den tidigare antagna *skadade zonen* och har, liksom vid borrningen av deponeringshålen och initial upphettning, skapats antingen av rörelser i existerande mikrosprickor, eller som ett resultat av utvidgning eller bildning av nya mikrosprickor i redan existerande skadat område.

Frekvensen av lokaliserade händelser har generellt varit låg jämfört med när temperaturen först ökade 2003 och när de snabba tryckförändringarna inträffade i december 2004. Ett lågt antal AE antyder att bergmassan har stabiliserats. Trots en snabb temperaturökning under denna mätperioden är antalet AE fortfarande lågt och i överensstämmelse med tidigare observationer. Trycket minskade snabbt i september 2005 när man öppnade ett dränage till tunneln. Dränaget stängdes igen ungefär två månader senare, vilket ledde till en snabb tryckökning. Detta verkar inte ha haft någon betydande inverkan på antalet eller fördelning av AE runt deponeringshålet. Detta skiljer sig från resultaten från december 2004, då en snabb tryckökning ledde till 32 händelser som uppstod i kluster under en period av två dagar. Händelserna som noterades då tolkades som spänningsförändringar i berget eftersom det svarar mot den snabba tryckförändringen. Detta inducerar små rörelser i redan existerande mikrosprickor, eller leder till att nya mikrosprickor i den svagare bergmassan bildas. Trots att man lokaliserat ett kluster av händelser under de senaste 6 månaderna så har inte tryck- och temperaturförändringarna orsakat en tillräcklig omfördelning av spänningar så att ytterligare mikrosprickor bildats.

Contents

Table of Figures

Table of Tables

1 Introduction

This report describes results from acoustic emission (AE) and ultrasonic monitoring around a canister deposition hole (DA3545G01) in the Prototype Repository Experiment at SKB's Hard Rock Laboratory (HRL), Sweden. The monitoring aims to examine changes in the rock mass caused by an experimental repository environment, in particular due to thermal stresses induced from canister heating and pore pressures induced from tunnel sealing. Monitoring of this volume has previously been performed during excavation [*Pettitt et al.*, 1999], and during stages of canister heating and tunnel pressurisation [*Haycox and Pettitt,* 2005a,b]. This report relates to the period between 1st October 2005 and 31st March 2006, and is the second of an ongoing 6-monthly processing and interpretation of the results for the experiment.

The Prototype Repository Experiment (Figure 1-1) has been designed to simulate a disposal tunnel in a real deep repository for disposal of high-level radioactive waste. Its objective is 'to test and demonstrate the integrated function of the repository components under realistic conditions on a full scale and to compare results with models and assumptions'. The experiment consists of a 90m long, 5m diameter sub-horizontal tunnel excavated in a dioritic granite using a Tunnel Boring Machine (TBM). The rock mass has two main discontinuous sets of sparse, en-echelon fractures [*Patel et al.*, 1997]. The Prototype Repository design incorporates six full-scale canister deposition holes which have been excavated vertically into the floor of the tunnel using a TBM converted to vertical boring. Each deposition hole measures 1.75m in diameter and approximately 8.8m in length. Simulated waste canisters, encased in a bentonite buffer, have been placed into each deposition hole and heated from within by specially designed electric heaters to simulate disposed radioactive material at elevated temperatures. The tunnel was then backfilled using a mixture of bentonite and crushed rock, and sealed using concrete plugs. A range of measurements are made in and around the tunnel and deposition holes. Pressure and temperature results, since a permanent array was installed, are summarised in Figure 1-2.

AE and ultrasonic monitoring is a tool for remotely examining the extent and severity of damage and disturbance around an excavation. This can be induced by the excavation method itself; by the redistribution of stresses (loading or unloading) resulting from the void or by environmental effects such as heating, saturation or pressurisation. Acoustic techniques are particularly adept at assessing the Excavation Damaged or Disturbed Zone (EDZ) as they allow it to be mapped spatially and temporally with high resolution, and they allow the effect on the rock mass to be quantifiably measured. Furthermore, acoustic techniques allow investigations to be conducted remotely, without the need for potentially damaging coring. *Young and Pettitt*[2000] give a review of AE and ultrasonic results from a number of experiments conducted in different underground environments.
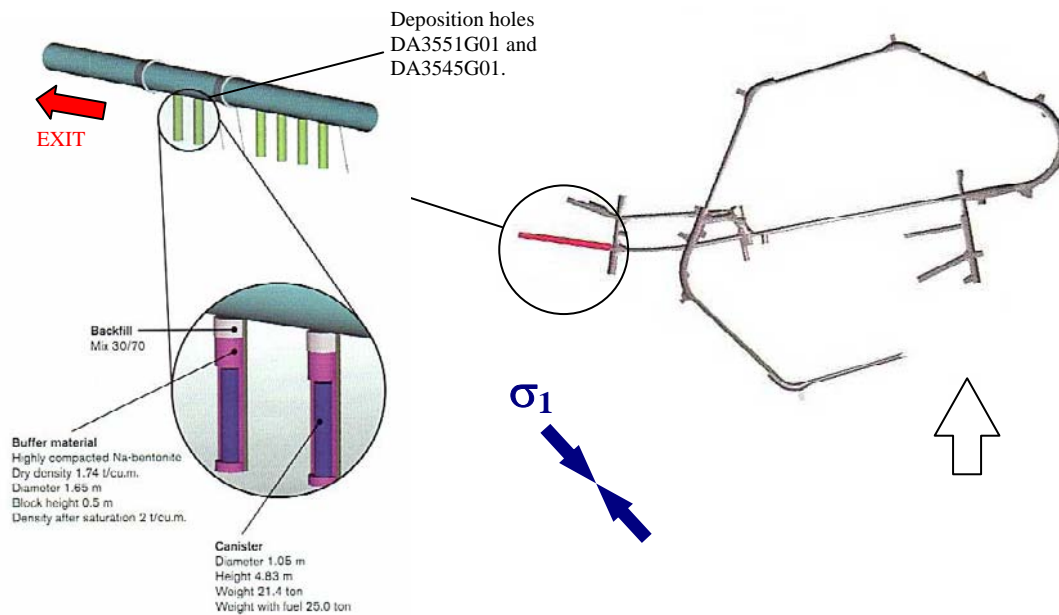
Figure 1-1: *Plan view of the experimental tunnels at the Äspö HRL and the location of the Prototype Repository. A schematic illustration of the final experimental set up is shown with canisters and bentonite clay buffer installed in the 1.75m diameter deposition holes. Note the entrance of the tunnel is towards the left. Graphics are modified from SKB[1999].*

- AE monitoring is a 'passive' technique similar to earthquake monitoring but on a much smaller distance scale (source dimensions of millimetres). AEs occur on fractures in the rock sample when they are created or when they move. The data acquisition system triggers on AEs when they occur and records full-waveform information that can then be used to delineate the amount, time, location and mechanism of fracturing.

- Ultrasonic surveys are used to 'actively' examine the rock. In this case an array of transmitters sends signals to an array of receivers. Amplitude and velocity changes on the ray paths can be interpreted in terms of changes in the material properties of the rock. Calculations using the velocities can determine the dynamic moduli, Young's modulus and Poisson's ratio, to give direct indications of the properties of the rock through which the raypaths travel. Crack density and saturation can also be calculated to determine changes in crack properties in the damaged and disturbed zones.

Detailed descriptions of the data acquisition and processing methodology are presented in Appendix I. The ultrasonic array consists of twenty-four ultrasonic transducers configured as eight transmitters and sixteen receivers installed into four instrumentation boreholes using specially designed installation frames sealed within slightly expansive grout. The array is designed to provide good coverage for AE locations and provide 'skimming' ray paths so as to sample the rock immediately adjacent to the deposition hole wall. ASC's InSite Seismic Processor [*Pettitt et al*., 2005], has been used to automatically process both the AE and ultrasonic survey data. Appendix II A and Appendix II B give the processing parameters used. Data from daily ultrasonic surveys has been automatically picked and arrivals cross-correlated to a reference survey for high-precision measurements of P- and S-wave velocity change through the experiment. Arrivals of AEs have been manually picked and three dimensional source locations have been calculated.
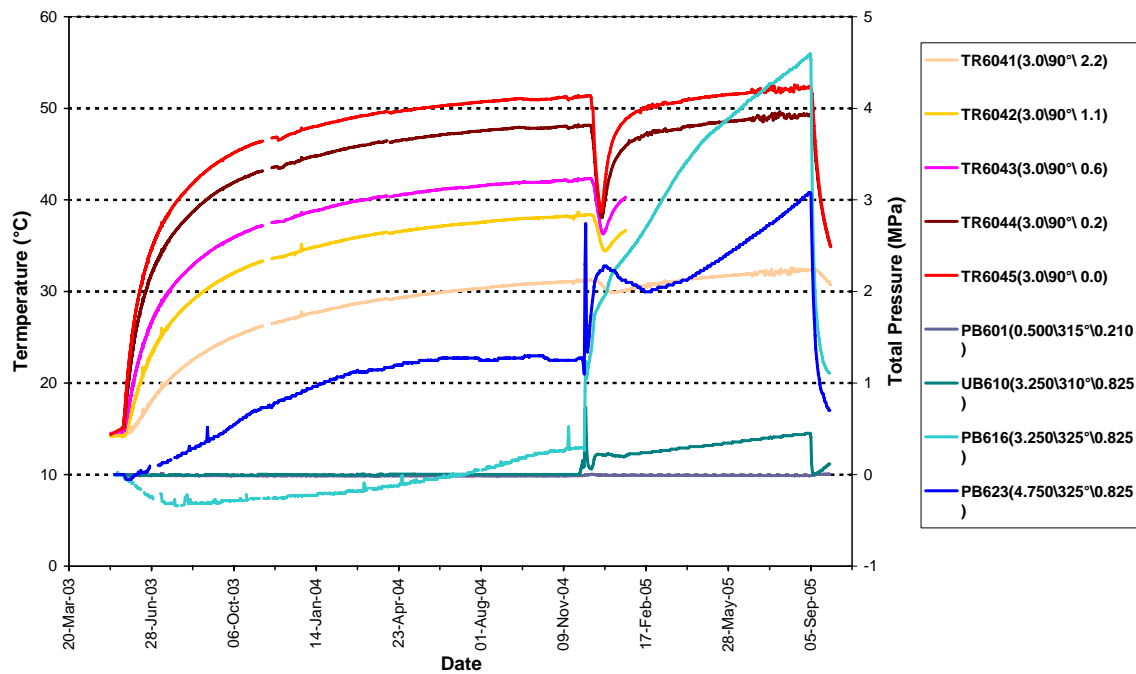
Figure 1-2: *Temperature (TR instruments) measured in the rock adjacent to the deposition hole and total pressure (PB and UB instruments) measured on the rock wall. Total pressure is the sum of pore pressure and bentonite swelling pressure [Goudarzi, 2005].*

2 Specific Objectives

This six-month period of ultrasonic monitoring in the Prototype Repository Experiment, has been undertaken with the following objectives:

- Produce accurate source locations for AEs so as to delineate the spatial and temporal extent of any brittle microcracking within the rock mass around the deposition hole and locate any movements on pre-existing macroscopic fractures.

- Conduct regular ultrasonic surveys to assess the effect of heating and other environmental changes on the velocity and amplitude of transmitted ultrasonic waves.

- Investigate changes in dynamic moduli and crack density to show how the properties of the rock volume around the deposition hole change through the experiment.

- Relate the AE and ultrasonic measurements to the measured *in situ* stress regime and other operating parameters such as temperature and fluid pressure.

- Outline how the results from this reporting period relate to previous monitoring periods, and into the overall experimental aims and objectives.

3 Ultrasonic Monitoring of the Prototype Repository

Ultrasonic monitoring has been conducted at the Prototype Repository in some form since September 1999. During excavation, monitoring of both deposition holes in section 2 (DA3551G01 and DA3545G01) was undertaken to delineate zones of stress related fracturing and quantitively measure fracturing in the damaged zone [*Pettitt et al.*, 1999]. Thereafter, monitoring has been undertaken on a single deposition hole (DA3545G01), and the response of the surrounding rock to changes in temperature and pressure has been measured. The previous report by *Haycox and Pettitt*[2005b] was the first of an ongoing 6-monthly processing and interpretation of the results. This report presents new results from the period 1st October 2005 to 31st March 2006. Further details of the ultrasonic monitoring are shown in Table 3-1 and described below.

Table 3-1: Summary of ultrasonic monitoring at the Prototype Repository to-date. Response Periods are defined in Section 5.

Report	Monitoring Period		Location		Response Period
Pettitt et al.[1999]	25/08/1999 18/09/1999	to	DA3551G01 DA3545G01	and	Excavation
Haycox and Pettitt[2005a]	20/03/2003 09/10/2003	to	DA3545G01		1
	29/04/2004 31/03/2005	to	DA3545G01		1, 2
Haycox and Pettitt[2005b]	01/04/2005 30/09/2005	to	DA3545G01		2, 3

A temporary ultrasonic array was installed around the rock volume when deposition hole DA3545G01 and its neighbour DA3551G01 were first excavated in September 1999 [*Pettitt et al.*, 1999]. A total of 2467 AE triggers were obtained during monitoring of the two deposition holes. Of these 1153 were located. There was significantly more AE activity around the second deposition hole (labelled DA3545G01) than the first (DA3551G01). This difference is likely to depend upon intersection of the excavation with a greater number of pre-existing fractures. These fractures may be preferentially located in the side wall of the deposition hole or preferentially orientated to the *in situ* stress field. Fracturing associated with excavation-induced stresses was observed with AEs distributed mainly in regions orthogonal to the maximum principal stress, σ_1. This was consistent with observations from the Canister Retrieval Tunnel and from dynamic numerical models. AEs, and hence microcrack damage, were shown to locate in clusters down the deposition hole and not as a continuous 'thin skin'. *Pettitt et al.*[2000] showed that these clusters were associated with weaknesses in the rock mass generated by excavation through pre-existing fractures. Damage in the side wall of the deposition holes depended significantly on these pre-existing features. The *in situ* stress field was a contributing factor in that induced stresses were sufficiently high to create damage in these weakened regions although not sufficiently high to create significant damage in the rock mass as a whole.

A permanent ultrasonic array, with transducers grouted into instrumentation boreholes, was installed in the rock mass in June 2002. In this arrangement, ultrasonic monitoring has been conducted between 20th March and 9th October 2003, and then from 29th September 2004 to the present. The gap in monitoring occurred when the ultrasonic acquisition system was used for another experiment in the HRL (Pillar Stability Experiment). Processing and reporting of results has been undertaken by *Haycox and Pettitt*[2005a] and *Haycox and Pettitt*[2005b] and is further discussed in Section 5. A description of instruments measuring other environmental factors (such as temperature and pressure) and their locations can be found in *Goudarzi and Johannesson*[2006].

4 Results

4.1 Ultrasonic surveys

Figure 4-1 shows the three-dimensional velocity structure for the survey recorded on 8th December 2004. This was used as the reference survey for processing ultrasonic results for the previous monitoring period, after a rapid change in pressure in the deposition hole occurred on 4th December 2004. This particular survey was chosen because it has high quality signals, which enables the highest number of raypaths to be processed. This reference survey is also used during this reporting period. Raypaths passing through the deposition hole have been removed.

Between 16th February 2006 and 9th March 2006 amplitudes on receiver 7 are observed to decrease to very low levels. Consequently, determining velocities using the cross-correlation technique is very difficult as this technique works by comparing changes between waveforms of similar character. Therefore, raypaths involving receiver number 7 have been discounted from the analysis of velocity and amplitudes. From the 10th March signals have improved and been consistent until the end of the reporting period.

Measurements from temperature and pressure instruments located in, and around, the deposition hole provide an indication of the major environmental changes occurring during this reporting period. The temperature in the rock around the deposition hole is shown in Figure 4-2. The heaters in canister 6 (deposition hole DA3435G01), were turned off on 5th September 2005 [*Johannesson*, 2005], resulting in a decrease in temperature around the deposition hole. On 3rd November 2005, the heaters were switched on and temperature is observed to increase again. Initially this change is shown by sensors TR6045 and TR6055 (i.e. the nearest to the canister) but occurs on most sensors within three days. A rapid increase in temperature is observed initially. By the end of the monitoring period, a maximum temperature of 51.3°C is reached, with a rate of increase of approximately 0.1°C per week.

Figure 4-3a shows total pressure in the tunnel backfill above the deposition hole. Pressure in the deposition hole is displayed in Figure 4-3b. A slow rate of increasing pressure is displayed by the instruments in the backfill above the deposition hole (Figure 4-3a). A maximum of 0.5MPa is reached by sensor UFA15 by the end of the reporting period. The instruments located in the rock adjacent to the deposition hole, show the greatest variation (Figure 4-3b). From 1st November 2005 pressure is observed to increase. By 1st December, pressure has increased from 1.64 to 5.15MPa at PB616, and from 0.70 to 3.08MPa at PB623. After an initially rapid increase, pressure measured on these instruments increases at a relatively constant rate for the rest of the reporting period. Pressure increases for only 7 days on instrument UB610 before decreasing to a constant 0.4MPa. This instrument is located half way up the deposition hole in the bentonite buffer. It is understood that these variations are probably caused by changes in the buffer temperature (changes in the water volume caused by the temperature in combination with low hydraulic conductivity) [*Johannesson*, 2006].
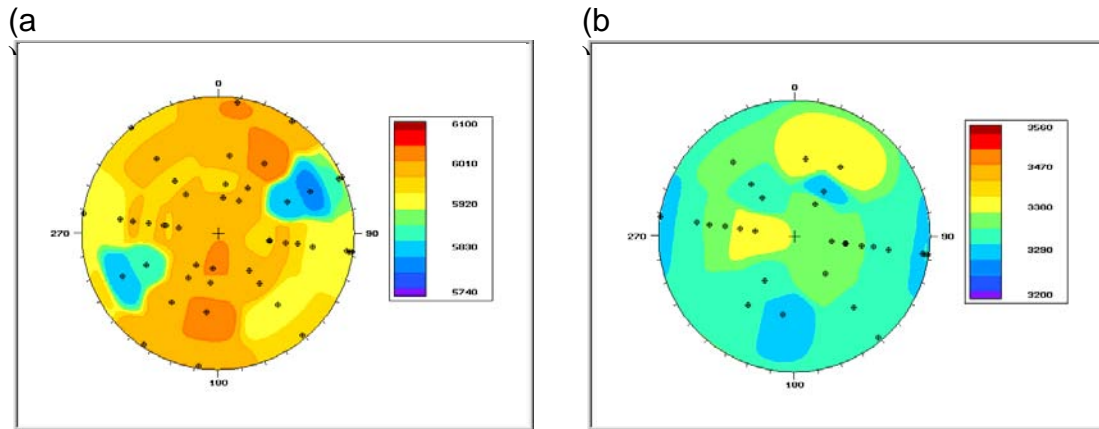
Figure 4-1: *Lower-hemisphere stereonets of a) P-wave velocity and b) S-wave velocity for the reference survey on 8th December 2004. The ray path orientations are shown by black markers.*

Velocity changes are measured between transmitter-receiver pairs on the daily ultrasonic surveys using a cross-correlation technique that allows a velocity resolution of ±2m.s⁻¹ (see Appendix I). Average P- and S-wave velocity change is shown in Figure 4-4. Over the first month velocity reduces at a consistent rate, P-wave velocity decreasing slightly faster than S-wave velocity. Between 2nd and 3rd November 2005 there is a drop in P-wave velocity of 1.5m.s⁻¹ and S-wave velocity of 0.5m.s⁻¹. This is a significant change, given that the average is determined from velocity measured on many raypaths. After the sudden drop, both P- and S-waves show increases in velocity of 3.4m.s⁻¹ and 1.8m.s⁻¹ respectively, such that by the end of the reporting period average velocity is slightly faster than at the start.

Further investigation of the sudden drop in velocity has been undertaken. This has confirmed that the change is "real" and not the result of an acquisition or processing artefact. Decreases in P-wave velocity are measured between the two days on 65 of the 76 possible raypaths. The magnitude of velocity change is small on individual ray paths, being generally of the order 1-3m.s⁻¹ (of the order of the estimated uncertainty in any one measurement). When averaged over the entire array these measurements produce a consistent and significant result. The greatest change is measured on transmitter 1 to receiver 16 which exhibits a decrease of 3.2m.s⁻¹ over the course of one day. Waveforms of surveys on 2nd and 3rd November have been compared for a selection of raypaths in order to confirm the result is not caused by a processing or acquisition artefact. An example is shown in Figure 4-5. A decrease in velocity is represented by a movement in the waveform to the right. There is also a small drop in average S-wave velocity on the same date, although this is smaller than the P-wave change. 40 raypaths increase in velocity from a possible 48, the largest drop of 1.5m.s⁻¹ occurring on raypath transmitter 8 to receiver 12.

Significantly, not all ray paths are affected in an identical manner, nor are ray paths purely from one instrumentation borehole to another affected. Consequently this change has been interpreted as a localized change in the general rock properties rather than a systematic change in the measurement devices used in the project. Average velocity change is compared in detail to temperature and pressure measurements in Figure 4-6. A small increase in total pressure is observed on 2nd November, however a larger

increase occurs on 3rd November. Temperature does not increase significantly until 4th November. Therefore, the sudden drop in velocity coincides with the pressure increase in the rock around the deposition hole. Stresses may be redistributed as this takes place causing a relatively sudden decrease in velocities. This is further discussed later in this section. A similar instance occurred in the previous monitoring period, when a jump took place between 13th and 14th September 2005. A velocity increase of 1-2m.s^{-1} was measured on this occasion, when pressure and temperature rapidly decreased. This is an interesting result which demonstrates that a step-wise change in velocity occurs immediately following a rapid change in pressure. Further discussion about this, and previous jumps in velocity, can be found in Section 5.
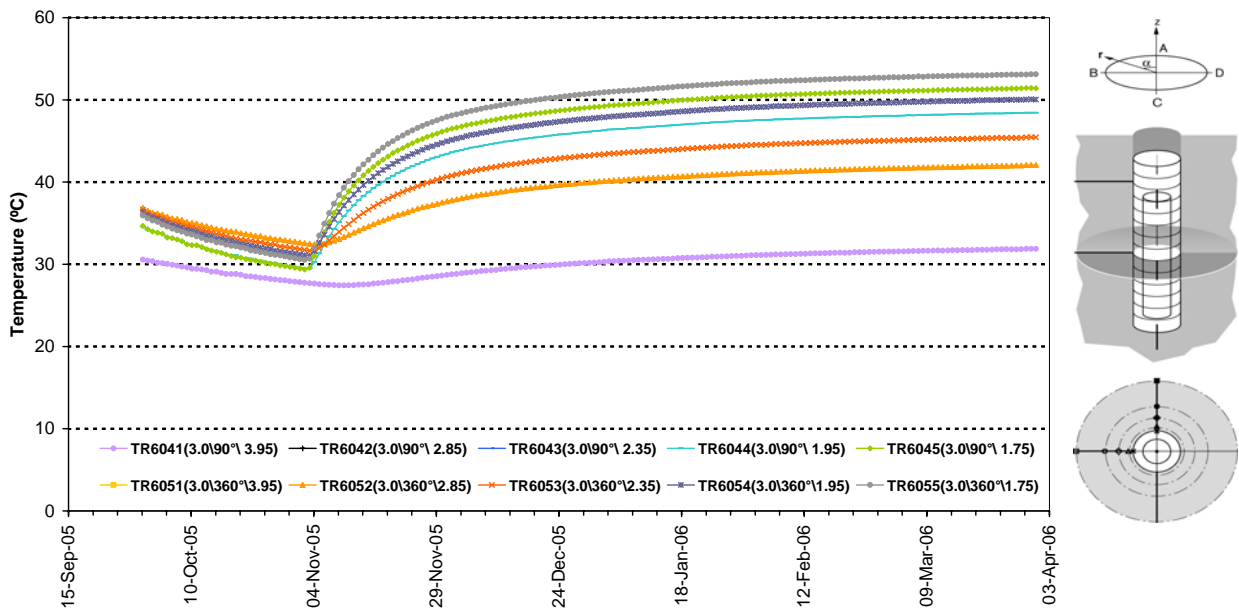
Figure 4-2: Temperature around deposition hole DA3545G01. The sensors are positioned mid-way up the deposition hole with different depths into the rock mass (see right-hand inset) [Goudarzi, 2006].

Figure 4-4b shows the average amplitude change measurements during this reporting period. For the first month, P- and S-wave amplitudes decrease at a relatively constant rate. Minimum amplitudes are reached on 6th November 2005, S-wave amplitude having reduced by 0.7dB or approximately 10%, whilst P-wave amplitude reduces by 0.6dB. After this date amplitudes rapidly increase, closely correlating with temperature and pressure measured around the deposition hole (see Figure 4-2). By the end of the reporting period, the P and S-wave amplitudes are slightly higher than at the start. The S-wave is shown to be slightly more responsive than P-wave.
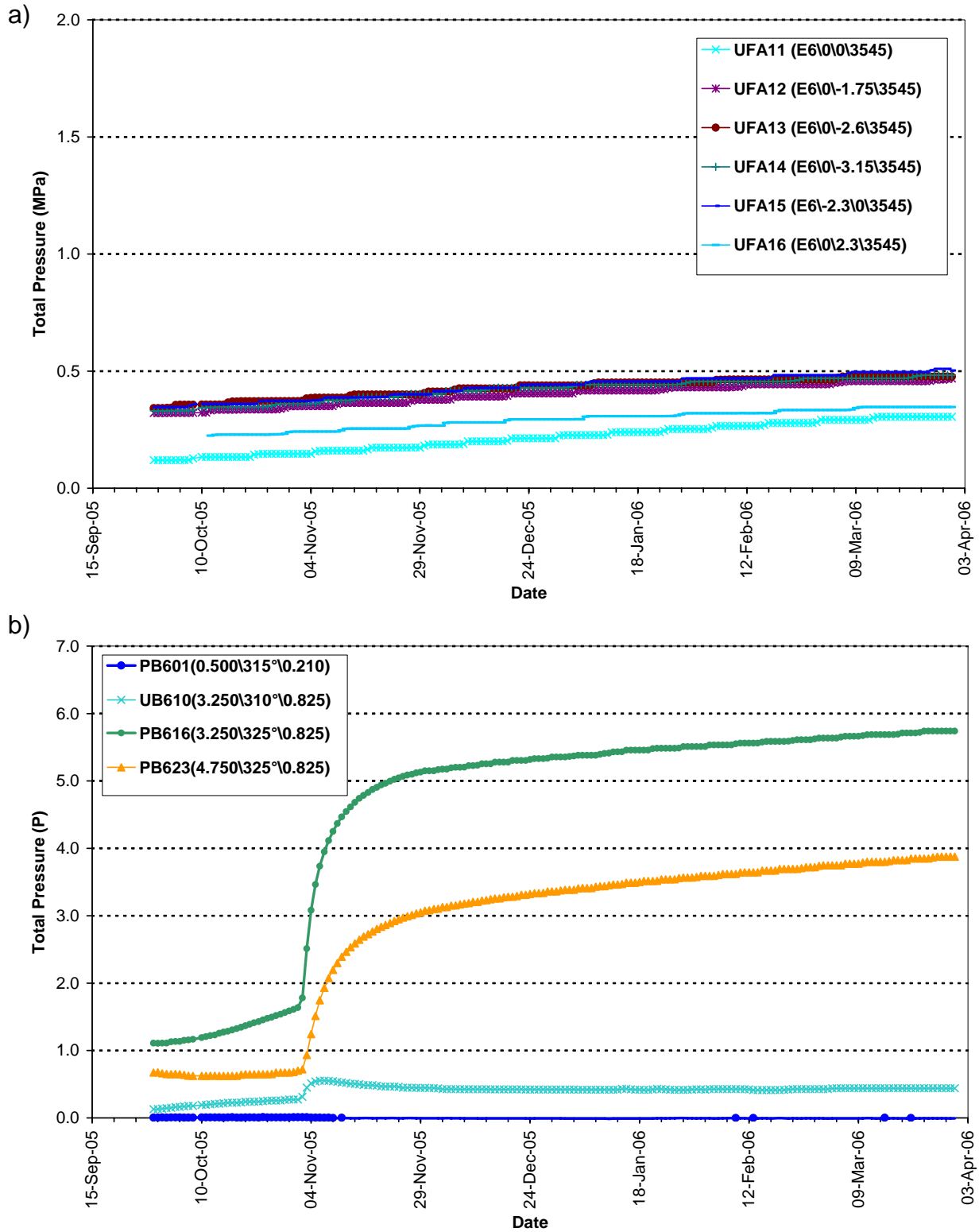
Figure 4-3: *Total pressure in (a) the backfill over deposition hole DA3545G01; and (b) in the rock adjacent to deposition hole DA3545G01 [Goudarzi, 2006]. The position of the sensors is presented in the figure legend as distance down, angle around and distance from the axis of the deposition*
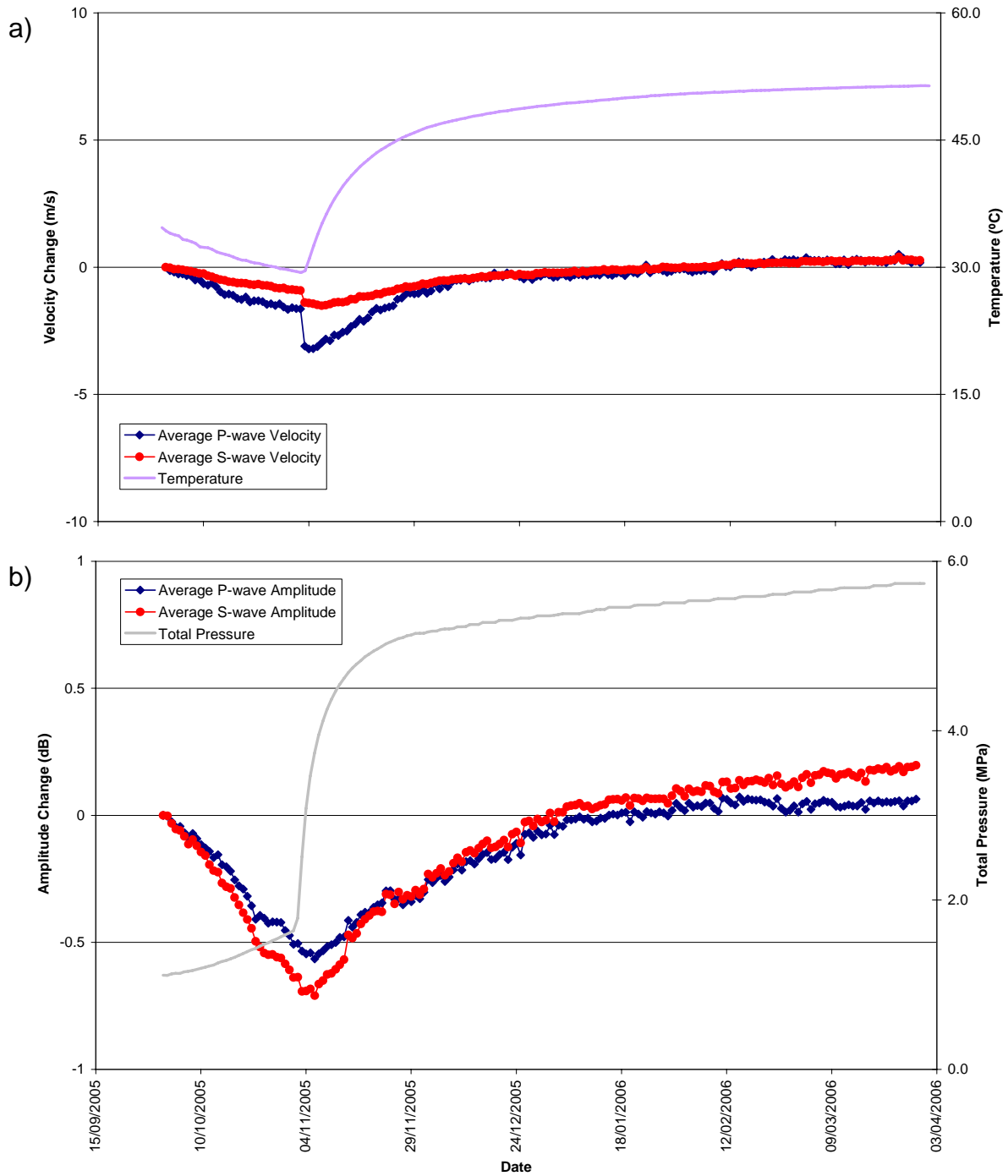
Figure 4-4: *Average P- and S- wave (a) velocity change and (b) amplitude change, for the reporting period. Temperature (TR6045) and total pressure (PB616) are displayed on the secondary axes.*
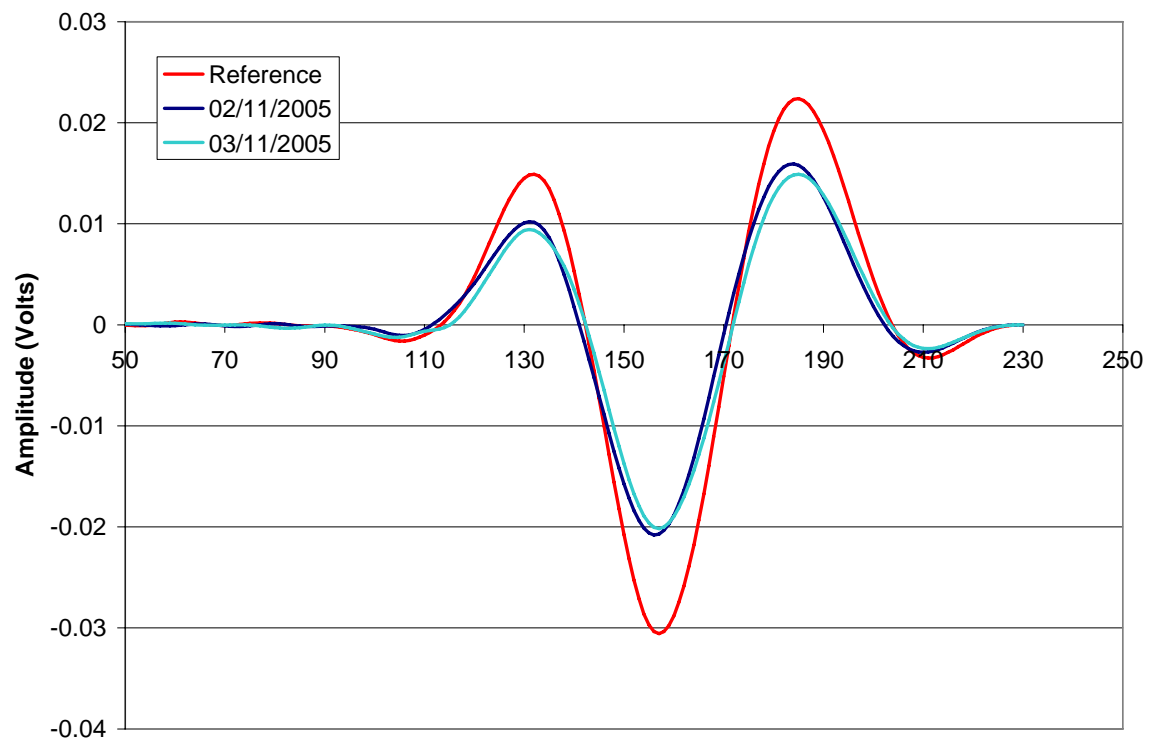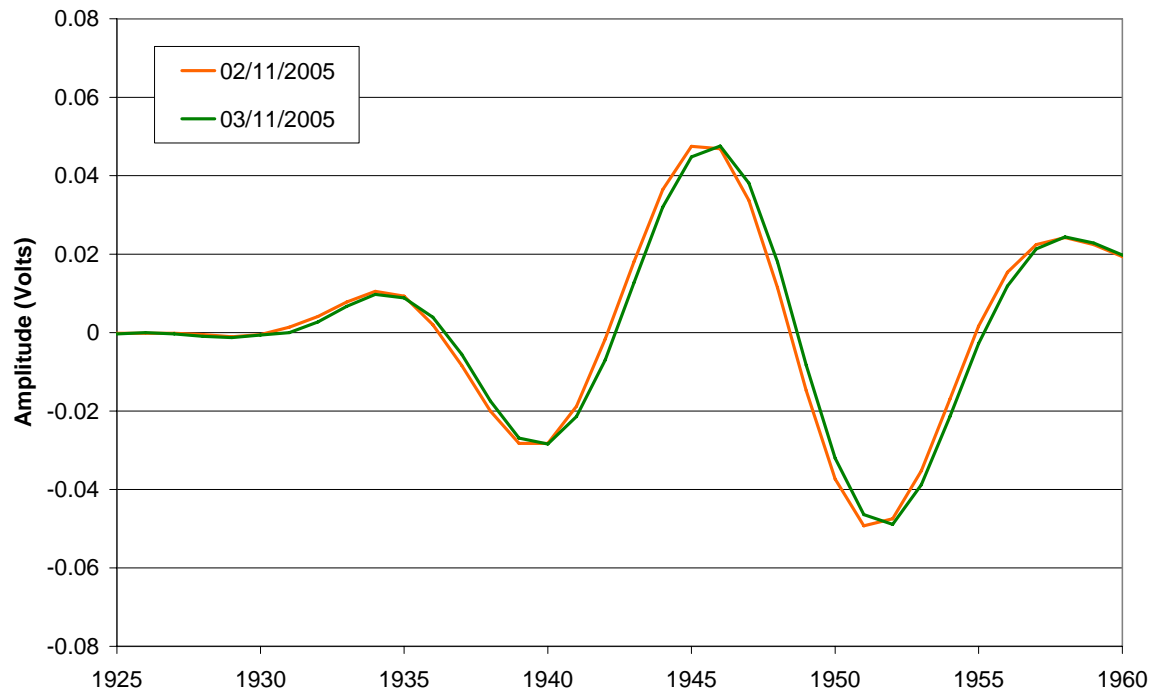
Figure 4-5: *Example plots of (a) raw waveform data points and (b) cross correlation windows for the raypath transmitter 7 to receiver 2 on 2ⁿᵈ and 3ʳᵈ November 2005. The second plot also shows the reference survey from 8ᵗʰ December 2004.*
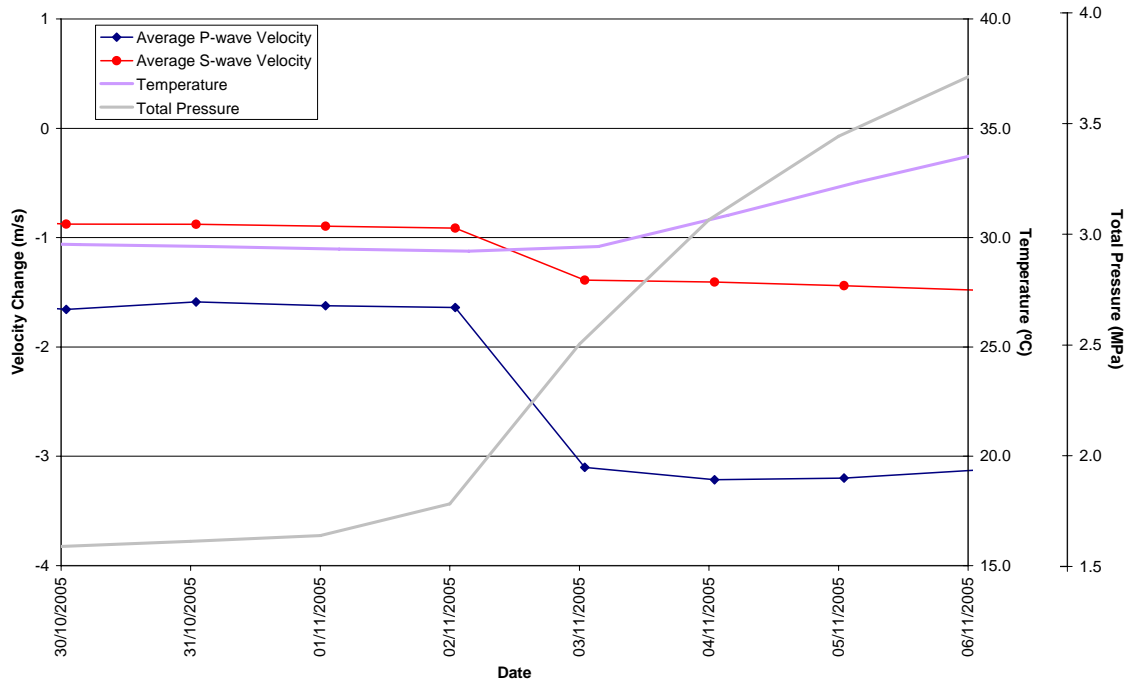
Figure 4-6: Detailed view of the sudden drop in velocity that occurs between 2nd and 3rd November 2005. Average P- and S- wave velocity change are displayed on the primary axis. Temperature (TR6045) and total pressure (PB616) are displayed on the secondary axes.

The raypaths from the ultrasonic surveys are categorised into six types by *Pettitt et al.*[1999], depending on their orientation with respect to the deposition hole and the in situ stress field (Figure 4-7). An interpretation of the ultrasonic results in terms of disturbed and damaged regions around the excavation void, from the excavation phase of the experiment, is also shown in this figure. *Pettitt et al.*[2000] undertook three-dimensional elastic stress modelling to describe these zones of stress.

Velocity changes measured on raypaths in the 'S3' category, during the monitoring period reported here, are presented in Figure 4-8. These raypaths pass within centimetres of the deposition hole through the excavation damage zone, in a region of low compressive or tensile stress. The particular raypaths have been chosen to provide a comparison of velocity variation down the deposition hole. Each plot is accompanied by a schematic diagram, on the right of the chart, which give a perspective of the region though which each of the raypaths pass. The three plots of raypaths passing closer to the bottom of the deposition hole (Figure 4-8b,c,d) all show similar patterns of velocity change, whereby velocity decreases during the first month, then increases afterwards, although the extent of the change varies down the borehole. The raypath passing closest to the top of the borehole exhibits little change in velocity. This raypath was also the least affected during heating [*Haycox and Pettitt*, 2005a,b]. The rock at this depth is above the top of the canister (which is situated between 449 and 454m depth), and thus it does not undergo changes in temperature to the same extent as lower raypaths.

Velocity results for raypath category 'S1' are displayed in Figure 4-9. These raypaths pass through a region of high compressive stresses and permanent damage close to the tunnel wall imaged by relatively high AE activity during excavation. During this period of monitoring, velocity on these raypaths does not change to the same extent as for

those of the 'S3' category. The greatest change is exhibited on transmitter 8 to receiver 6. By the end of the first month, a reduction in P-wave velocity of $10m.s^{-1}$ is recorded. Over the remaining five months of this reporting period, velocity increases by $20m.s^{-1}$. The other raypaths show a similar pattern but change to a lesser extent. Very little change in velocity is measured on the uppermost raypath, similar to that described above.

Figure 4-10 and Figure 4-11 compare the results of average velocity and amplitude changes across the different raypath categories described in Figure 4-7. P-wave velocity shows a greater change than S-wave velocity. Raypath category 'S3' exhibits the greatest variation with P-wave velocity reducing by $7m.s^{-1}$ by 5th November 2005. Between 5th November 2005 and 31st March 2006 P-wave velocity then increases by $13m.s^{-1}$ on this raypath. These values are $3m.s^{-1}$ and $5m.s^{-1}$ respectively for S-wave velocity. Similar patterns are shown on 'S1' and 'C1', and to a lesser extent on 'C2'. These changes are of low magnitude (not more than $5m.s^{-1}$), which is small in comparison to changes of up to $25m.s^{-1}$ that occurred during the heating phase (up to 5th September). Interestingly, velocity on the 'far' raypath category does not decrease during the first month of this reporting period. After the sudden drop occurs, the velocity remains constant throughout the remaining time. Amplitudes are observed to decrease in the first month, then increase for the remaining time for both P- and S-waves. For P-wave amplitude 'C1' shows the largest decrease initially. By the end of the monitoring period amplitudes have returned to the levels at the start, except for category 'C2' which ends 0.57dB higher for P-wave and 0.66dB higher for S-wave amplitude.
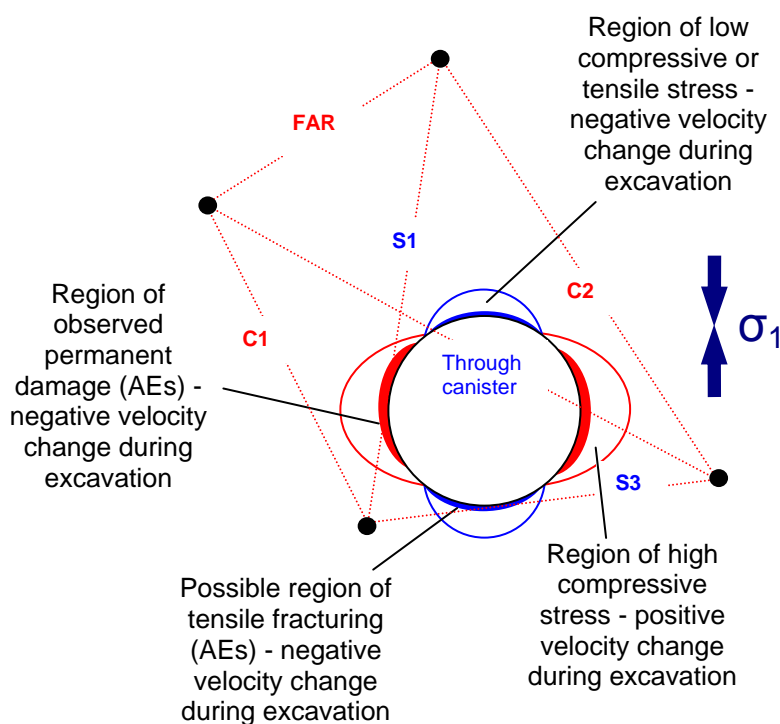
Figure 4-7: Interpretation of the ultrasonic results during excavation in terms of disturbed and damaged regions around the deposition hole. Zones of induced stress are inferred from elastic modelling and the σ_1 orientation. After Pettitt et al.[1999].

The largest increase in velocity is for category 'S3' raypaths, but the largest increase in amplitude occurs on 'C2' raypaths. 'S3' raypaths pass through an area of fractured rock adjacent to the deposition hole in which microcracks are under tensile stress. 'C2' raypaths are not highly fractured, but have been observed previously to be affected elastically by changes in pressure and temperature. An increase in velocity is expected to bring about a similar response in amplitude, however this is not the case in this example. In this study, both temperature and pressure change at the same time and these may cause different effects on velocities and amplitudes. A more detailed study could focus on which of these is more sensitive to temperature or pressure.

Figure 4-12 shows changes in Young's Modulus, Poisson's Ratio, Crack Density and Saturation parameters calculated from the average measured velocities for the ray path categories. 'Crack Density' and 'Saturation' of the rock mass are determined using the method of *Zimmerman and King*[1985], as described in Appendix 1. Young's Modulus decreases when the rock is de-pressurised and temperature is decreased (indicating a reduction in stiffness of the rock mass). Least affected, is the 'Far' raypath category. 'S3' category shows the largest reduction of approximately 0.2%. When temperature and pressure start to increase the stiffness of the rock increases, particularly on 'S3'. Crack density increases during the first month, following on from previous monitoring where cooling and pressure reduction has led to microcracks reopening. When pressure and temperature increase, the crack density reduces, particularly on 'S3' raypath category.

The initial reduction in the stiffness of rock around the deposition hole, and increase in crack density, is a continuation of conditions that existed at the end of the previous monitoring period. The response is interpreted as an opening of existing microfractures and pore spaces in the region of tensile fracturing. This may be the result of a cooling of the rock and reduction in pressure from the deposition hole interior, returning the rock to a state prior to heating when microfractures were more open. When temperature and pressure increase, the associated increase in stiffness and decrease in crack density can be interpreted as the closing of existing microfractures and pore spaces. Existing microcracks in the low-compressive or tensile region were initially unloaded immediately after excavation. Consequently they are more reactive to stress changes than in the compressive region where stresses act to pre-close the microcracks. Large changes were also observed on this category when heating commenced. Increasing thermal stresses, acting on the rock around the deposition hole once more, now cause microfractures to close again.

The sudden drop in velocities observed between 2nd and 3rd November 2005 can be interpreted in terms of a change in rock properties using the results displayed in Figure 4-12. It is recognised that the sudden drop occurs immediately after drainage to the tunnel is closed, causing pressure to increase around the deposition hole. There appears to be a similar magnitude of response to this event by all raypath categories. A decrease in Young's Modulus occurs which indicates a reduction in stiffness of the rock. This short term change is therefore likely to be a sudden reaction of the rock mass to the increase in pressure, perhaps caused by a general opening of microcracks caused by increased pore pressures. The long term trend is to then close these microcracks from increased thermal stresses. Further work is required to de-couple the response temperature and pressure change. The sudden change in pressure is not accompanied by an increase in the rate of AE or trigger activity indicating no further damage is occurring to the rock.
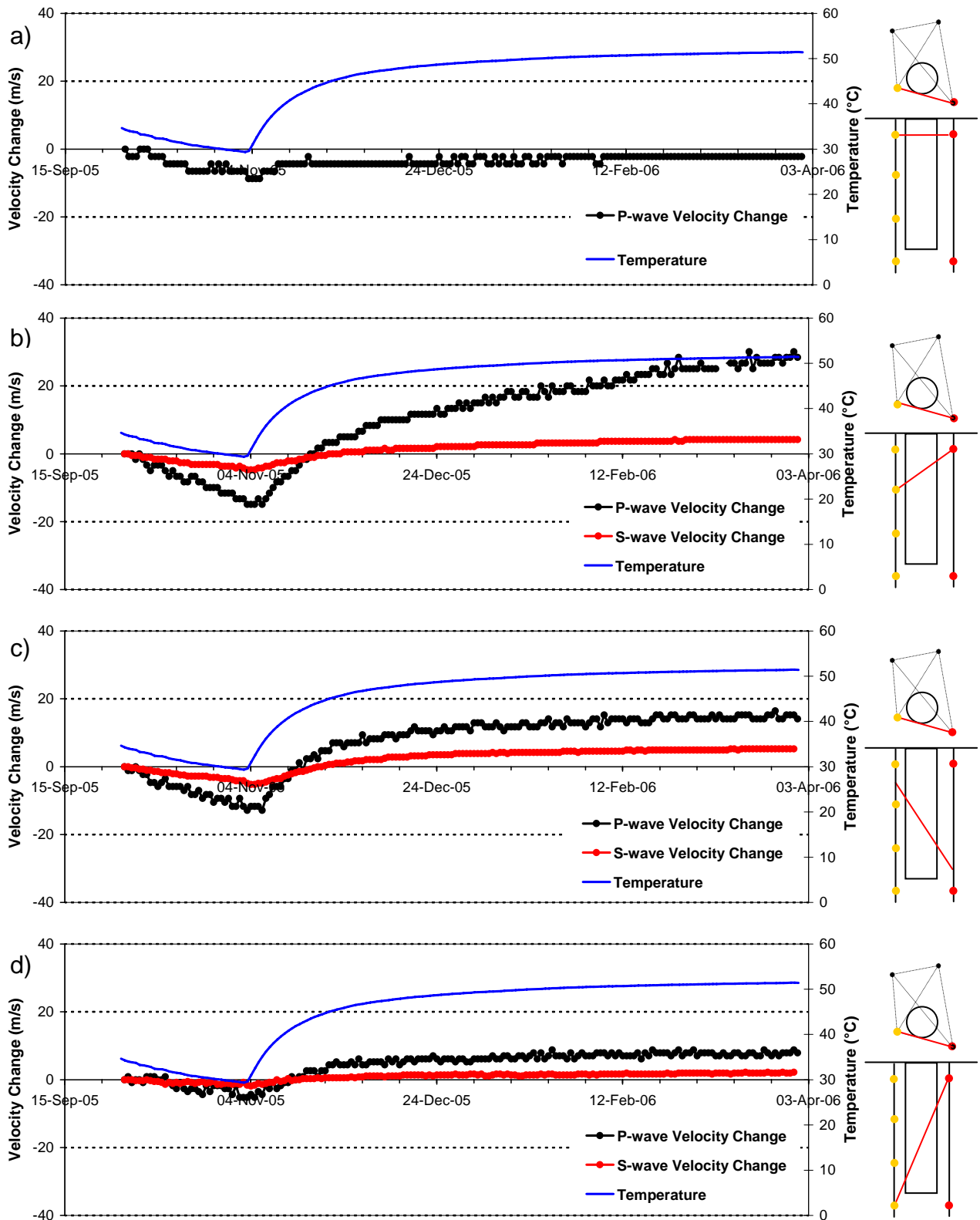
Figure 4-8: *Velocity changes measured on ray path category 'S3' (Figure 4-7) for deposition hole DA3545G01. Ray paths shown are from a top transmitter to receivers with increasing depth: a) transmitter, $t_n=1$, receiver, $r_n=5$; b) $t_n=1$, $r_n=6$; c) $t_n=2$, $r_n=6$; d) $t_n=4$, $r_n=1$. Schematic diagrams in the right margin indicate the relative locations of transmitter (red) and receiver (gold). Temperature (TR6045) is displayed on the secondary axes.*

36
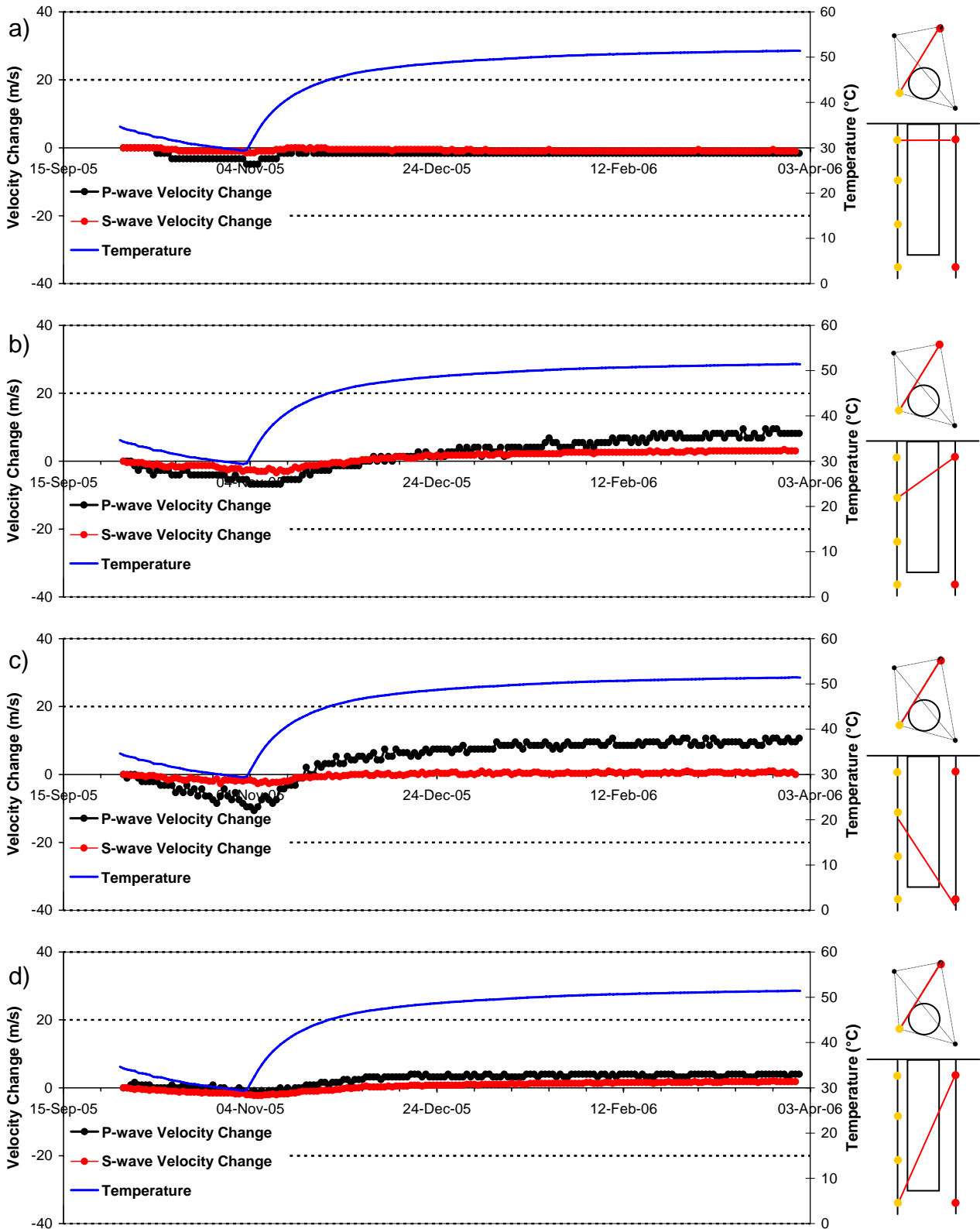
Figure 4-9: Velocity changes measured on ray path category 'S1' (Figure 4-7) for deposition hole DA3545G01. Ray paths shown are from a top transmitter to receivers with increasing depth: a) transmitter, tn=7, receiver, rn=5; b) tn=7, rn=6; c) tn=8, rn=6; d) tn=7, rn=8. Schematic diagrams in the right margin indicate the relative locations of transmitter (red) and receiver (gold). Temperature (TR6045) is displayed on the secondary axes.

37
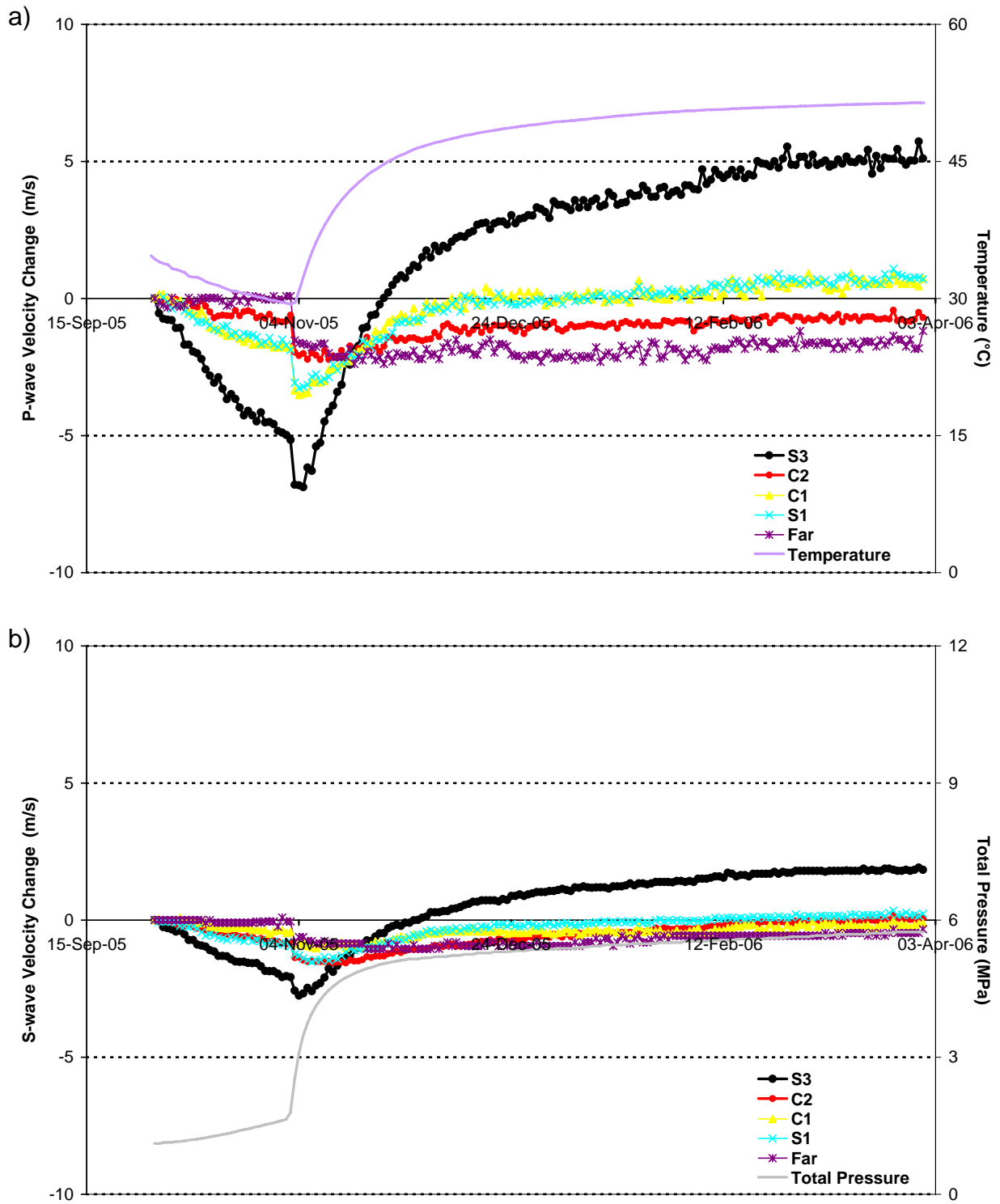
Figure 4-10: Velocity change plots of 5 raypath categories around deposition hole DA3545G01 for (a) P-waves and (b) S-waves. Temperature (TR6045) and total pressure (PB616) are displayed on the secondary axes.
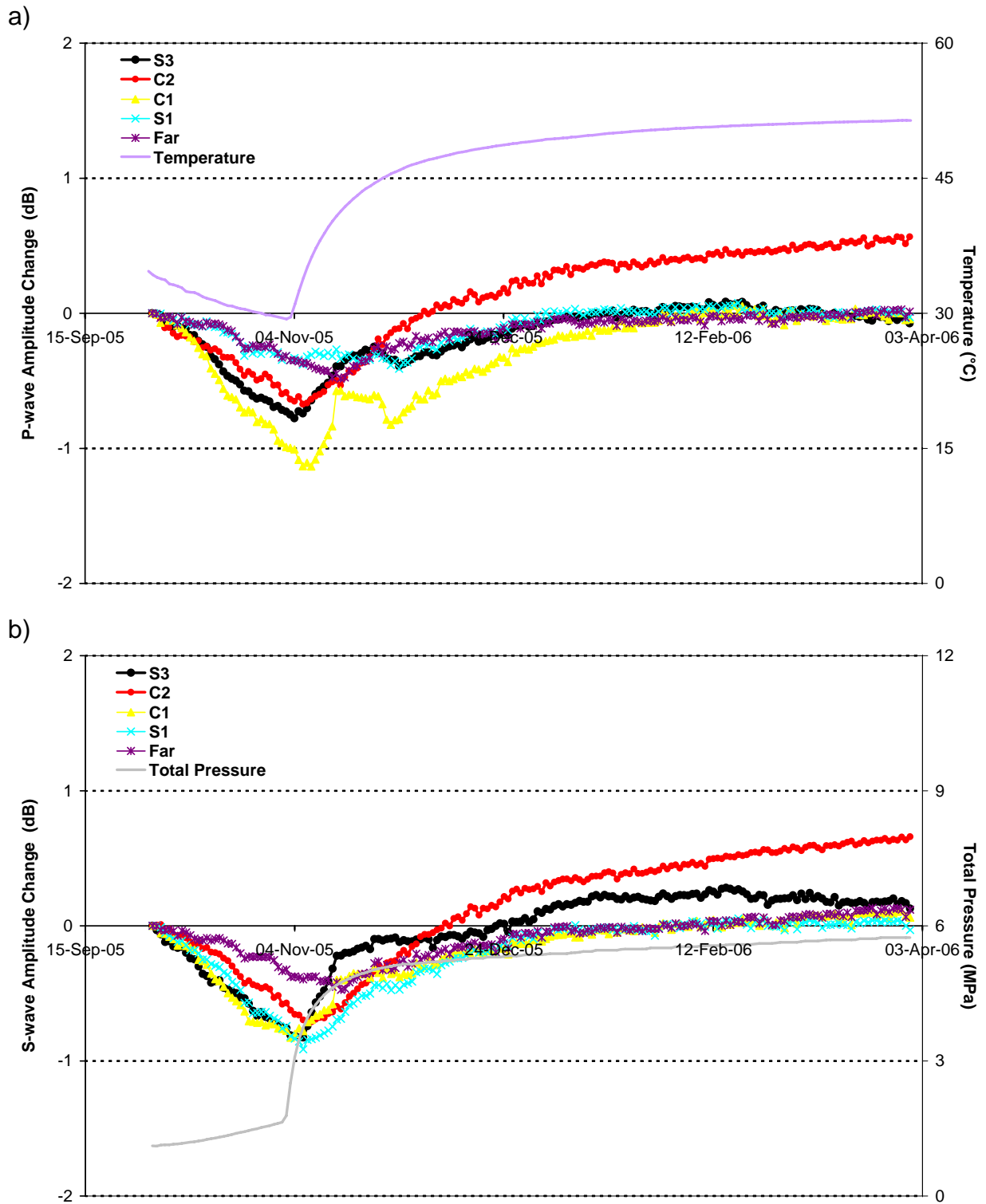
Figure 4-11: *Amplitude change plots of 5 raypath categories around deposition hole DA3545G01 for (a) P-waves and (b) S-waves. Temperature (TR6045) and total pressure (PB616) are displayed on the secondary axes.*
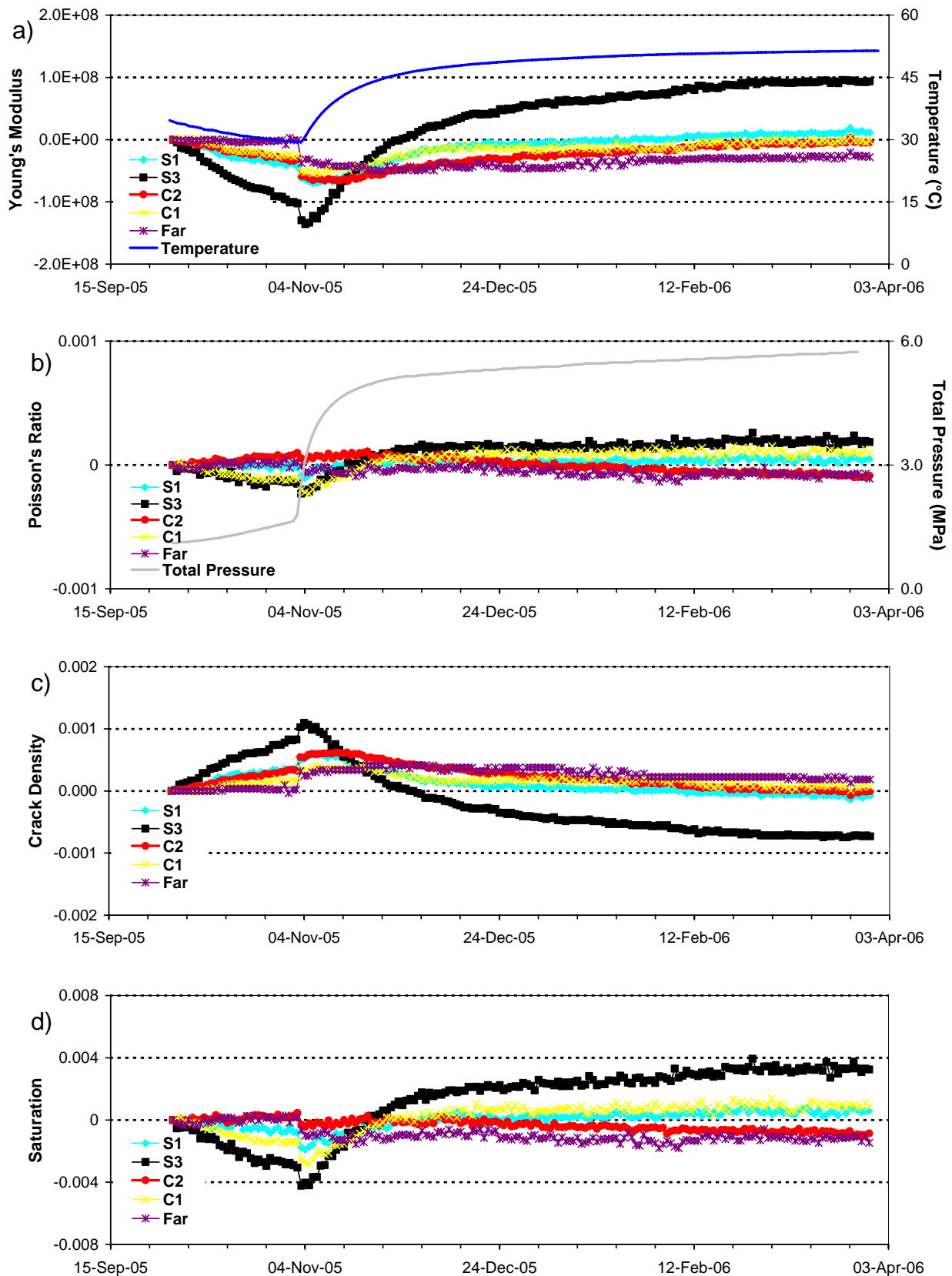
Figure 4-12: *Modulus during this reporting period for average P- and S-wave velocity values on different raypath orientations. (a) Young's Modulus, (b) Poisson's Ratio, (c) Crack Density and (d) Saturation. Raypath orientations are described in Figure 4-7. Temperature (TR6045) and total pressure (PB616) are displayed on the secondary axes.*

4.2   Acoustic Emissions

Processing of acoustic emissions has been undertaken following the procedures outlined in Appendix I. 50 events have been located with high confidence from 100 triggered events recorded during this period. Estimated uncertainties on these events are of the order 10cm as described by calibration 'hits' performed within the deposition hole (see Appendix I for further details).

Figure 4-13 shows the temporal response of the triggers and located events recorded during this monitoring period. A trigger is described as an event that has been acquired by the system, but may not be of sufficient quality to be located during the processing procedure. 'Noise' events, produced from either electrical or man-made sources, have been removed from this count because they are not determined to be 'real' events. The temporal distribution of AE triggers, shown in Figure 4-13a, has two distinct peaks in activity with 18 triggers on 31st October 2005 and 10 triggers on 9th January 2006. These days have 18% of the 100 triggers recorded during this monitoring period. During the rest of the reporting period the rate of triggering remains relatively constant, with an average of 0.4 triggers per day. The temporal response of the 50 located AEs is displayed in Figure 4-13b. On a single day, no more than 2 AEs have been located. An average number of 0.27 events are recorded per day. This is an increase on the previous six months (0.21 event per day), but lower than six months before (0.32 events per day). When compared to the high level of activity observed during excavation, in which up to 20 events per hour were recorded, this represents a very low level.

Three projections are presented in Figure 4-14 to show the spatial distribution of located AEs. The deposition holes and tunnel are represented by blue wire frame. The instrumentation boreholes are represented by brown vertical lines. The majority of the events locate in the immediate vicinity of deposition hole DA3545G01. Three events also locate close to the neighbouring deposition hole DA3551G01. Figure 4-15 shows the waveforms of selected events in order to demonstrate the high quality data collected. A cluster of 39 events (see i in Figure 4-14) is situated on the SE side of deposition hole DA3545G01 at a depth of 455.1m in a region of low-compressive or tensile stresses.

Figure 4-16 compares plan views of the activity during excavation, the first period of heating and this reporting period. In previous monitoring periods, the majority of events were distributed in the NE and SW quadrants which coincide with regions of increased compressive stress as imaged during excavation and initial stages of heating [*Pettitt et al.*, 2000; *Pettitt et al.*, 2002, *Haycox et al.*, 2005a]. Smaller clusters were observed in orthogonal regions of low-compressive or tensile stress. The events observed during this reporting period are consistent with these previous results with events locating in regions of previous activity. The events are therefore interpreted as a continuation of activity in the previously imaged damage zone and, similar to during excavation and initial heating, are created either by movement on pre-existing microcracks, or as a result of extension or formation of new microcracks in the existing damaged region.

a)

b)
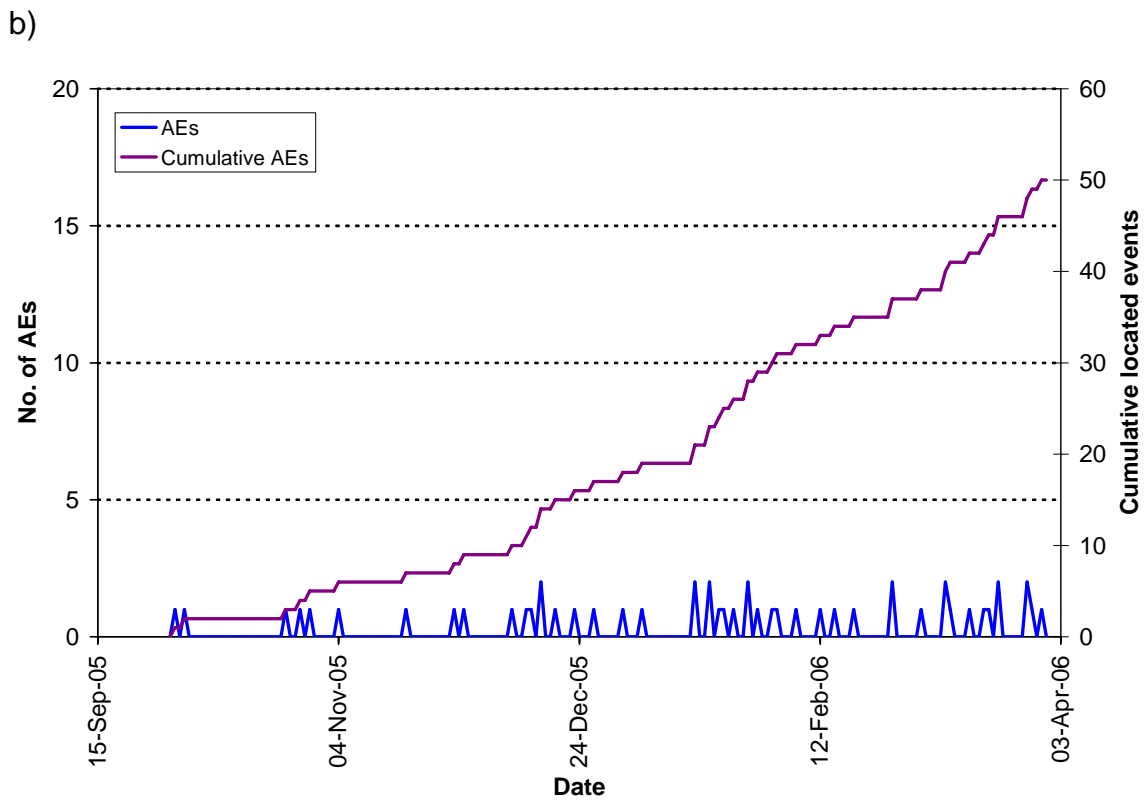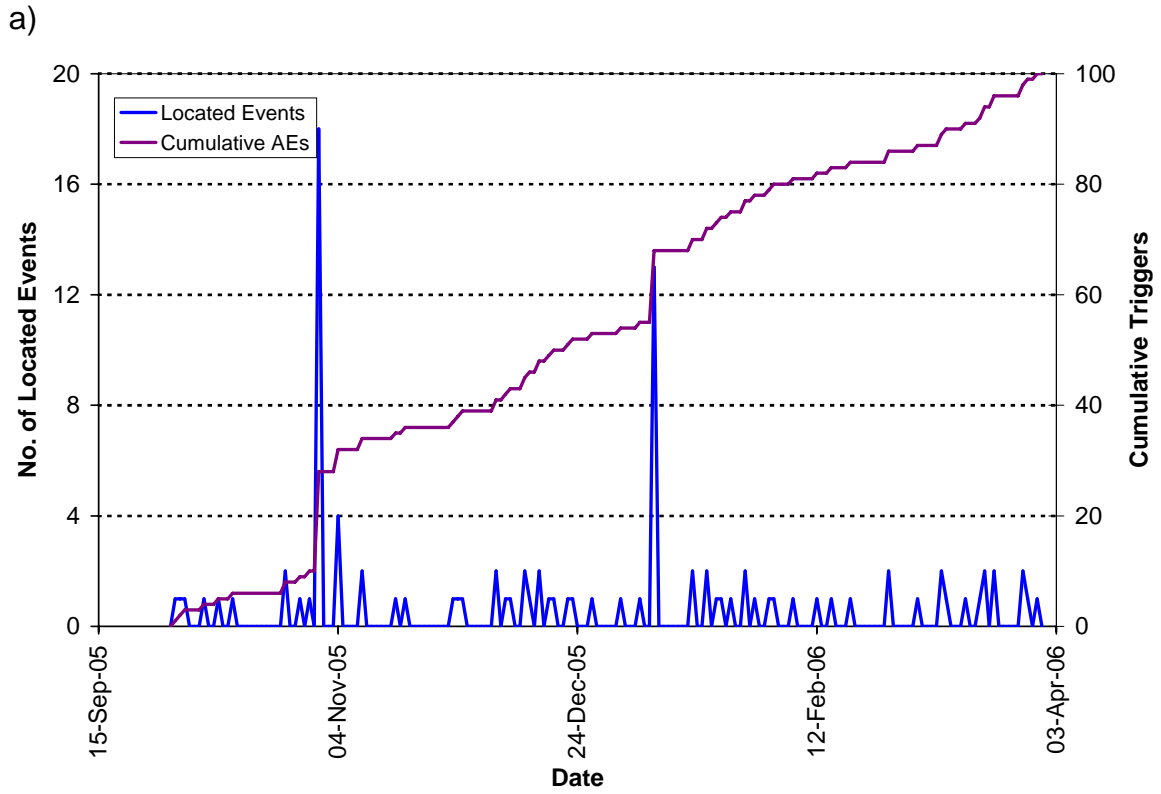
Figure 4-13: *Temporal response plot of (a) AE triggers and (b) located AEs; number per day on left axes and cumulative number right hand axes.*
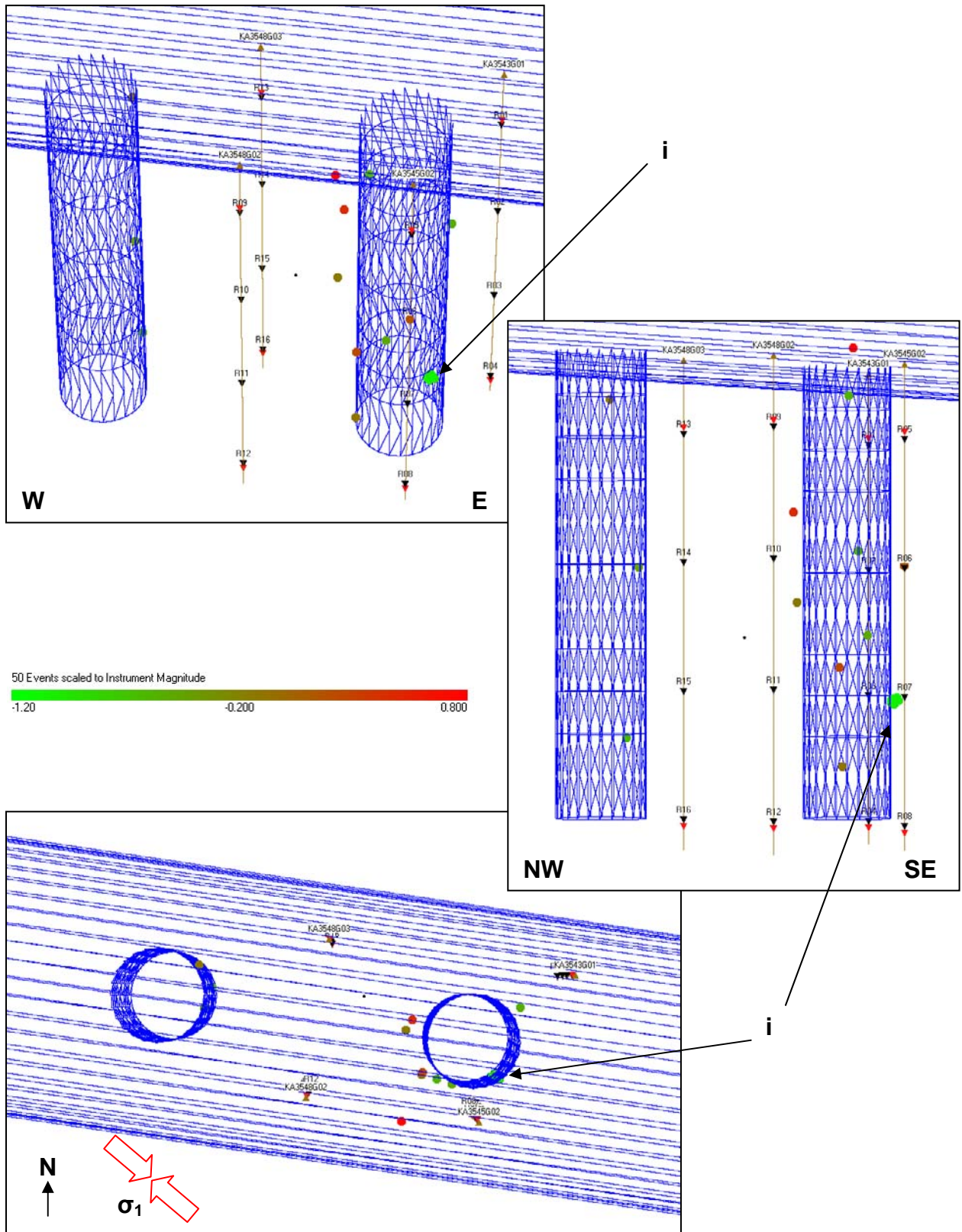
Figure 4-14: *Three views of AE activity located around deposition holes DA3545G01 and DA3551G01. (Top: Oblique view looking North. Middle: Transverse view looking north. Bottom: Plan view).*
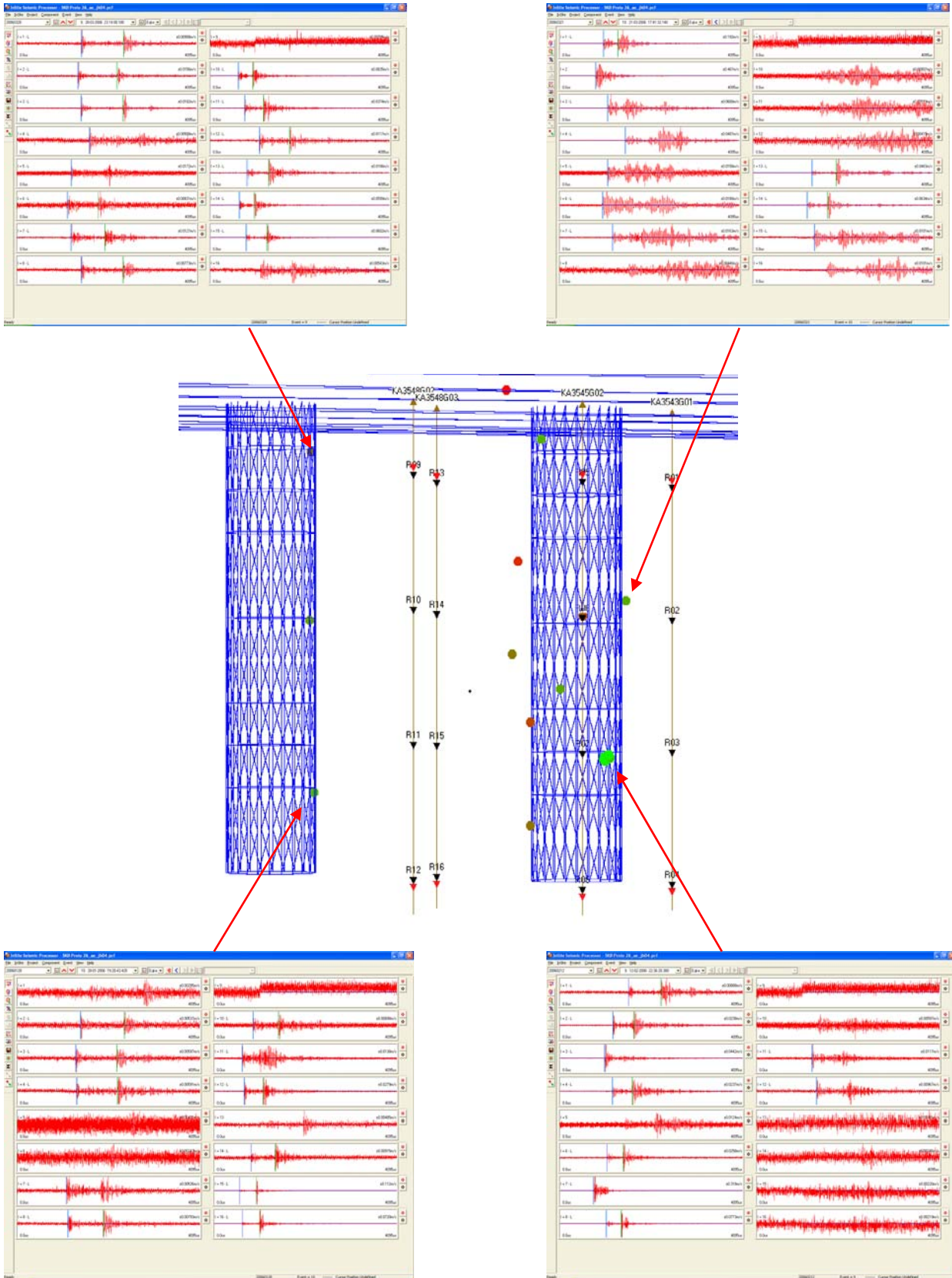
Figure 4-15: *Waveforms from selected events shown in relation to a transverse view of AE activity.*
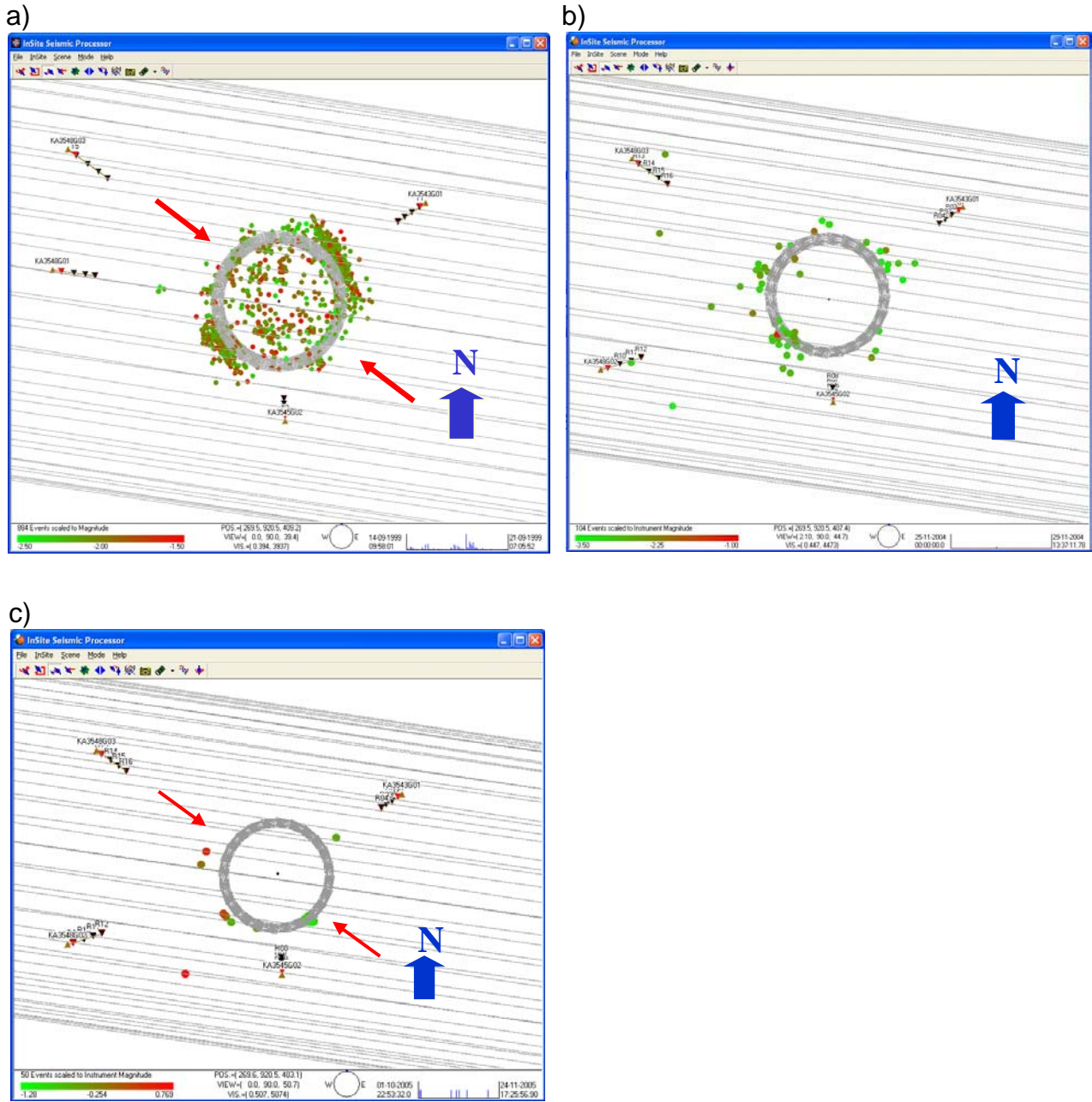
Figure 4-16: *Plan view of AEs located around deposition hole DA3545G01 during (a) the excavation phase, (b) the first monitoring phase during heating and (c) this reporting period. The red arrows mark the orientation of the principle stress.*

5 Summary of Monitoring to Date

This section of the report investigates how the results obtained during this reporting period relate to observations from previous monitoring of the Prototype Repository since the start of heating in March 2003. The experiment has been split into four periods for analysis based on environmental factors. The dates of these periods, together with a summary of temperature, pressure, velocity, amplitude and acoustic emissions, are presented in Table 5-1. Average velocity and modulus changes for the five raypath categories, described in the previous section, are presented in Figure 5-1 to Figure 5-6. These changes are summarised in schematic diagrams for each of the periods in Figure 5-9 to Figure 5-12.

In Period 1, temperature rose rapidly in the first few months after heaters in the canister were switched on. At this point in the experiment, pressure in the tunnel was very low and relatively constant. Average P-wave velocity increases by 16m.s^{-1} and S-wave velocity increases by 12m.s^{-1} during this period (Figure 5-1). A very similar response is exhibited by amplitudes, with P-wave amplitude increasing by 7dB and S-wave amplitude increasing by 10dB

All raypath categories show an overall increase in velocity during this period, albeit with different temporal responses. 'S3' raypaths passing though the low compressive or tensile region show the largest overall increase in velocity (25m.s^{-1} for P-wave and 10m.s^{-1} for S-wave). Raypath categories passing through the compressive zone exhibit less average increase (categories 'S1', 'C1', C2'). The 'S3' category passes through a volume that is unloaded and hence experiences low compressive stresses. This volume responds more rapidly to thermal stresses because existing microfractures are initially unloaded and hence more open than microfractures in the compressive region. P- and S-wave velocities decrease a similar amount during excavation as they increase during heating. This suggests very strongly that the microfractures induced in the regions of tensile damage around the deposition hole close when thermal stresses are applied. The difference in the rate of response between raypaths in the compressive categories was interpreted as a different magnitude of response of the microfractures in the rock mass to increasing thermal stresses.

In the first few months of heating, another effect is superimposed onto the rock's response to thermal stresses. This is measured as a reduction in P-wave velocities compared to S-wave velocities in the first few months of heating. This is particularly noticeable on 'S1' category in Figure 5-2, in which P-wave velocity decreases by about 3.5m.s^{-1} while S-wave velocity remains constant. A desaturation occurs on all raypath categories, other than 'S3'. This must be caused by a drying of the rock mass, in the zones experiencing high compressive stresses, as heat is applied to the rock (i.e. both temperature and pressure are acting to expel moisture). In the low-compressed, or tensile, region saturation increases during this period. This is probably caused by hot fluids expanding into the open microfracture fabric.

In the second period, pressure rose rapidly after drainage from the tunnel was closed. This resulted in damage to the canister and the heaters being temporarily switched off. Temperature around the deposition hole reduced rapidly, but started increasing again after 13days. Significant changes to the character of many recorded ultrasonic waveforms were observed as significant increases in signal quality. This suggests that as pressure increased in the rock surrounding the deposition hole, attenuation of the ultrasonic waves is significantly reduced meaning that they can pass more efficiently

through the rock medium. P- and S-wave velocity increase by 2.8m.s^{-1} and 4.1m.s^{-1} respectively in the ten days following the pressure increase. A similar short term increase in average amplitude is observed with a peak reached about 15 days after pressure started to increase. Although amplitudes then reduce slowly, P- and S-wave amplitudes remain approximately 2.2dB higher than from Period 1.

The extent of the velocity increase at the start of the second period (November and December 2004) varies across the raypath categories. For instance in terms of P-wave velocity, 'C2' only exhibits a change of 0.9m.s^{-1}, while 'S1' increases by approximately 5.5m.s^{-1} over 5 days. The pressure increase can be interpreted as increasing the stiffness of the rock with a corresponding decrease in crack density. The magnitude of increase is greater for 'S1' and 'S3' categories because the volumes through which they pass are close to the deposition holes and contain a higher proportion of microfractures in an excavation damage zone. The pressure increase acts as a confining pressure on the rock mass leading to a closure of the pre-existing microcrack fabric and so a reduction in crack density. We observe that only a relatively small pressure increase is sufficient to close this microcrack fabric in the volumes already under high compressive stresses, leading to an initially high rate of change in measured velocities followed by a constant level, even though pressures may keep increasing afterwards. From Figure 5-2 the required pressure increase is approximately 1.5MPa.

Another effect at this time is a rapid cooling of the rock when the heater inside the canister is switched off (for 13 days between 2nd and 15th December 2004), followed by warming as the rock is reheated. The majority of categories do not show a significant change in P- or S-wave velocity during this period. However, category 'S3' exhibits a decrease in P- and S-wave velocity followed by an increase that mirrors the rate at which temperature changes (Figure 5-3). This category was found to be the most sensitive to thermal stresses during the initial stages of heating. When the rock cools, thermal stresses acting in this volume of low compressive (or slightly tensile) stresses reduce causing unloading of the microcracks. Microcracks close again when the rock is reheated and thermal stresses increase.

The third period began in September 2005, when additional drainage from a permeable mat placed on the inner surface of the outer plug was opened, and heaters were switched off. This resulted in a cooling and de-pressurisation of the deposition hole. P-wave and S-wave velocity decrease by 2.3m.s^{-1} and 1.1m.s^{-1} respectively. Similarly, P- and S-wave amplitudes decrease by 0.8dB and 1.0dB respectively.

The change in velocity on most raypaths is generally very low. An exception to this is category 'S3'. Decreases of 4.3m.s^{-1} and 2.9m.s^{-1} are measured over this time for P- and S-wave velocity respectively. This category is observed as the most sensitive to thermal stresses. Pressure from within the deposition hole, caused by hydraulic pressure and swelling of the bentonite buffer, was determined to be the primary constraint on these changes. The pressure increase acted as a confining pressure on the rock mass leading to a closure of the pre-existing microcrack fabric and so a reduction in crack density. Only a relatively small pressure increase was sufficient to close this microcrack fabric in the volumes already under high compressive stresses. As temperature decreases, thermal stresses again reduce in this volume causing microcracks to reopen and resulting in an increase in crack density and reduced stiffness of the rock.

During the fourth period, heaters were turned back on once more causing temperature around the deposition hole to increase. Pressure increased rapidly again, probably caused by changes in the buffer temperature (changes in water volume caused by the

temperature in combination with low hydraulic conductivity) [*Johannesson*, 2006]. Velocity increases rapidly at first, then at a constant rate, following a similar pattern to the temperature and pressure. During this period, P-wave velocity increases by 2.8, and amplitude increases by 0.5dB. S-wave velocity increases by 1.2, and amplitude increases by 0.9dB.

Raypath category 'S3' exhibits the greatest variation during this period, with P-wave velocity increases by $13m.s^{-1}$ and $5m.s^{-1}$ for S-wave velocity. Similar patterns are shown on 'S1' and 'C1', and to a lesser extent on 'C2'. Velocity on the 'far' raypath category remains constant throughout the remaining time. When temperature and pressure start to increase the stiffness of the rock increases, particularly on 'S3'. This is accompanied by a reduction in crack density. The associated increase in stiffness and decrease in crack density can be interpreted as the closing of existing microfractures and pore spaces as observed previously.

At the start of periods 3 and 4 a sudden (over a few days), but relatively small change in velocity is observed, superimposed on the longer-term trends. These are related to rapid changes in fluid pressure; a decrease in Period 3, and increase in Period 4. For Period 3, an increase in Young's Modulus occurs which indicates a stiffening of the rock. This short term change is therefore likely to be a sudden reaction of the rock mass to the decrease in fluid pressure, perhaps caused by a general closing of microcracks caused by decreased pore pressures. The reverse is true for Period 4, when a pressure increase leads to a general opening of microcracks caused by increased pore pressures. This is different to long term trends from thermal stresses and general confining of the rock mass.

All AEs located since heating commenced are presented in Figure 5-7. The majority of the events located close to the deposition hole wall, within the first 20cm and were distributed in the NE and SW quadrants that coincided with regions of increased compressive stress induced by the interaction of the stress field with the excavation void. This activity was interpreted as stress disturbance of the rock mass, particularly around pre-existing macrofractures that commonly intersect the excavation, or microcracking in the immediate vicinity of the fractures.

Figure 5-8 gives a measure of the number of located AEs during different periods of the experiment. In the first period the number of acoustic emissions located is high. This occurs when the rock is heated for the first time. On average, about 0.5 events are located per day during this period. At the start of Period 2, a rapid pressure increase led to 32 events locating in clusters over the course of two days. This is the highest number located since the deposition holes were excavated. The events recorded are interpreted as stress changes in the rock as it responds to the sudden pressure change. This induces small scale movement on pre-existing microcracks, or induces new microfractures in weaker volumes of the rock. Pore pressure increases may also have assisted in inducing slip on pre-existing microfractures, by reducing the normal stress on the fractures. Over the rest of this period, as pressure continues to increase, fewer events are located.

Very few events have been located during Periods 3 and 4. A rapid decrease, and then increase, in pressure and temperature appears to have no significant affect on the number, or distribution of AEs around the deposition hole. A low number of AEs suggests the rock mass has stabilised. Pressure measured in the deposition hole has reached 5.7MPa on one instrument by March 2006. This results in a confining pressure being placed on the rock around the deposition hole and could explained the cessation in AEs as movement on macrofractures and microcracks is inhibited.

Table 5-1: Summary of velocity, amplitude and AE variation measured during four periods of temperature and/or pressure change.

Name / Date	Temperature/Pressure	Velocity	Amplitude	AE
PERIOD 1 25th May 2003 to 31st October 2004	Heaters in canister switched on causing an initially rapid change in temperature which gradually levels out to a constant increase. An increase of 35ºC is measured for an instrument in rock adjacent to the deposition hole. Pressure constant	Rapid increase in P- and S-wave velocity on 'S3' category. Other categories show increases but to a lesser extent. Initial decrease in P-wave velocity in comparison to S-wave velocity for all raypaths except for 'S3'.	Amplitudes increase over this period by between 3dB and 9dB for P-wave amplitude, and 7dB and 12dB for S-wave amplitude.	AEs do not start immediately after heating. This could be a Kaiser-type effect in which AE rate remains close to background level until stress increases above the largest previous value. Peak of 13 events located on 26th June 2003. Average Event Rate = 0.5 / day
PERIOD 2 1st November 2004 to 4th September 2005	Drainage to tunnel closed on 1st November. Pressure in tunnel increases. Pressure increases measured in the deposition-hole buffer between 3rd and 5th December. Damage observed on canister on 6th December so drainage reopened and heaters switched off. Power switched on 15th December.	Velocity increases measured close to the tunnel from 26th November. Larger increases measured on categories 'S1' and 'S3'.	Amplitude increases measured close to the tunnel from 26th November.	Relatively large number of events recorded in this period. Peak rate of 32 AEs on 4th and 5th December. Events locate in clusters in previously observed damage zone. Average Event Rate = 0.4 / day
PERIOD 3 5th September 2005 to 2nd November 2005	Additional drainage is opened in August 2005 leading to a decrease in pressure and temperature. Heaters turned off on 5th September	P- and S-wave velocities decrease on all raypath categories except 'far'.	P-wave amplitude decrease on all category raypaths.	Slight increase in event rate above background rate recorded in previous 5 months. Average Event Rate = 0.3 / day
PERIOD 4 3rd November 2005 to 31st March 2006	Pressure in tunnel increases. Constant increase in pressure in buffer above deposition hole. Heaters switched on again so temperature around deposition hole increases.	P- and S-wave velocities increase on all category raypaths. Larger increases measured on 'S3'.	P- and S-wave amplitude increase on the majority of raypaths.	Cluster of 39 events located on SE side of deposition hole. Similar rate of AE locations. Average Event Rate = 0.3 / day
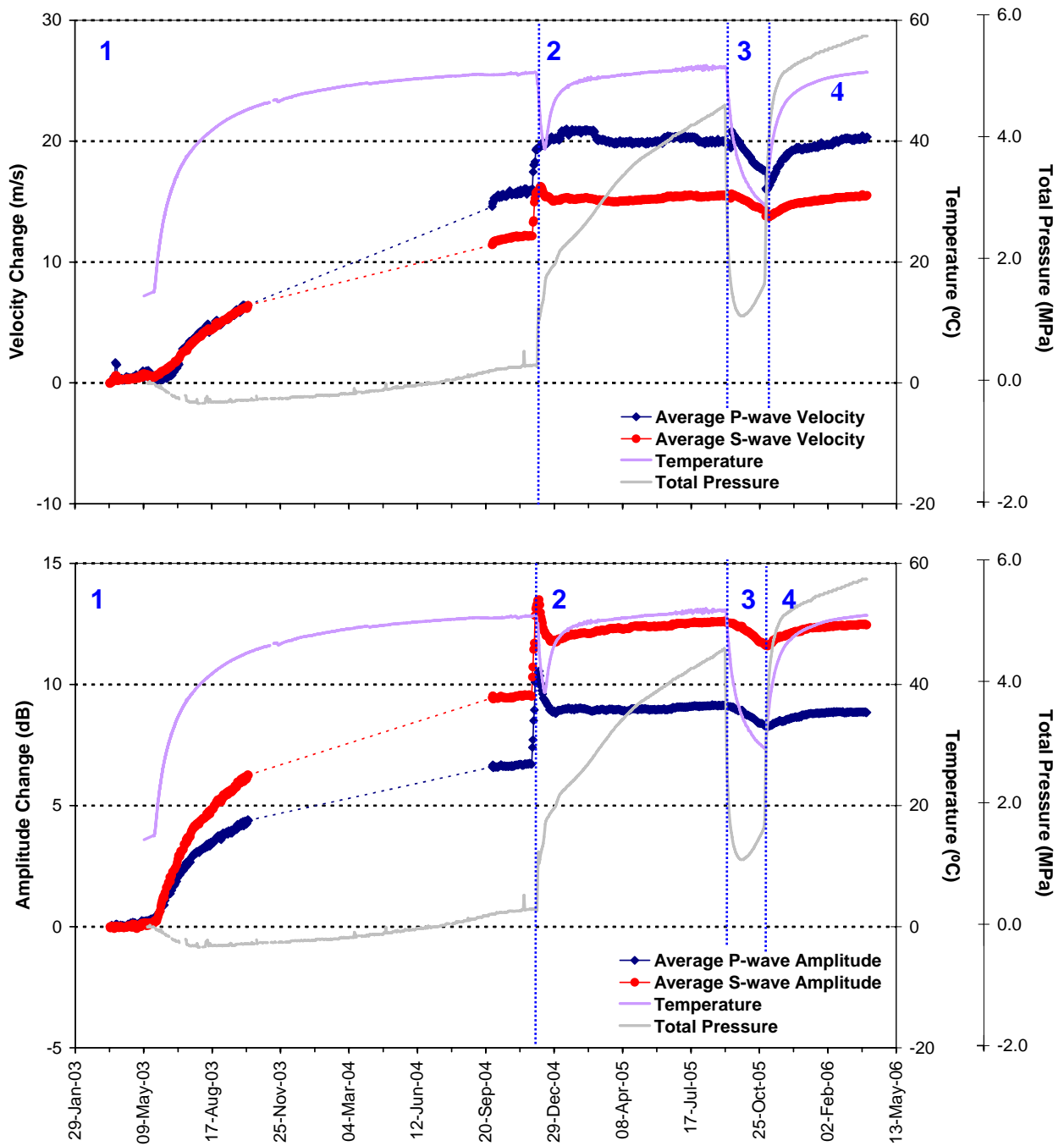
Figure 5-1: *P- and S-wave (a) velocity change and (b) amplitude change from the start of monitoring, plotted alongside temperature (TR6045) and pressure (PB616) measurements in deposition hole DA3545G01. The vertical blue lines differentiate between periods of similar environmental conditions (see Table 5-1).*
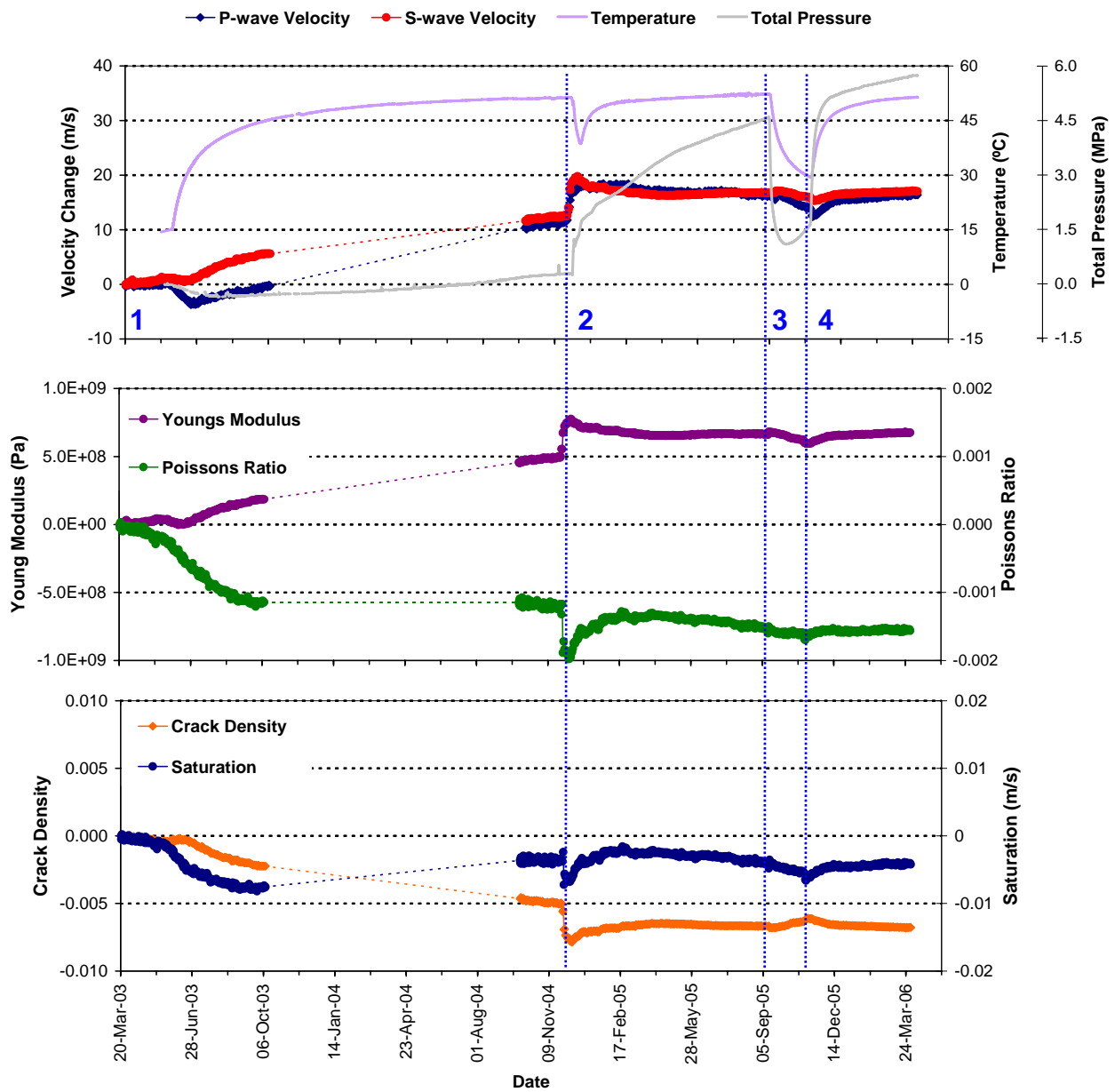
Figure 5-2: *Average P- and S-wave velocity change for raypaths on category 'S1' together with temperature (TR6045) and total pressure (PB616) (top), Young's Modulus and Poison's Ratio change (middle), and Crack Density and Saturation change (bottom).*
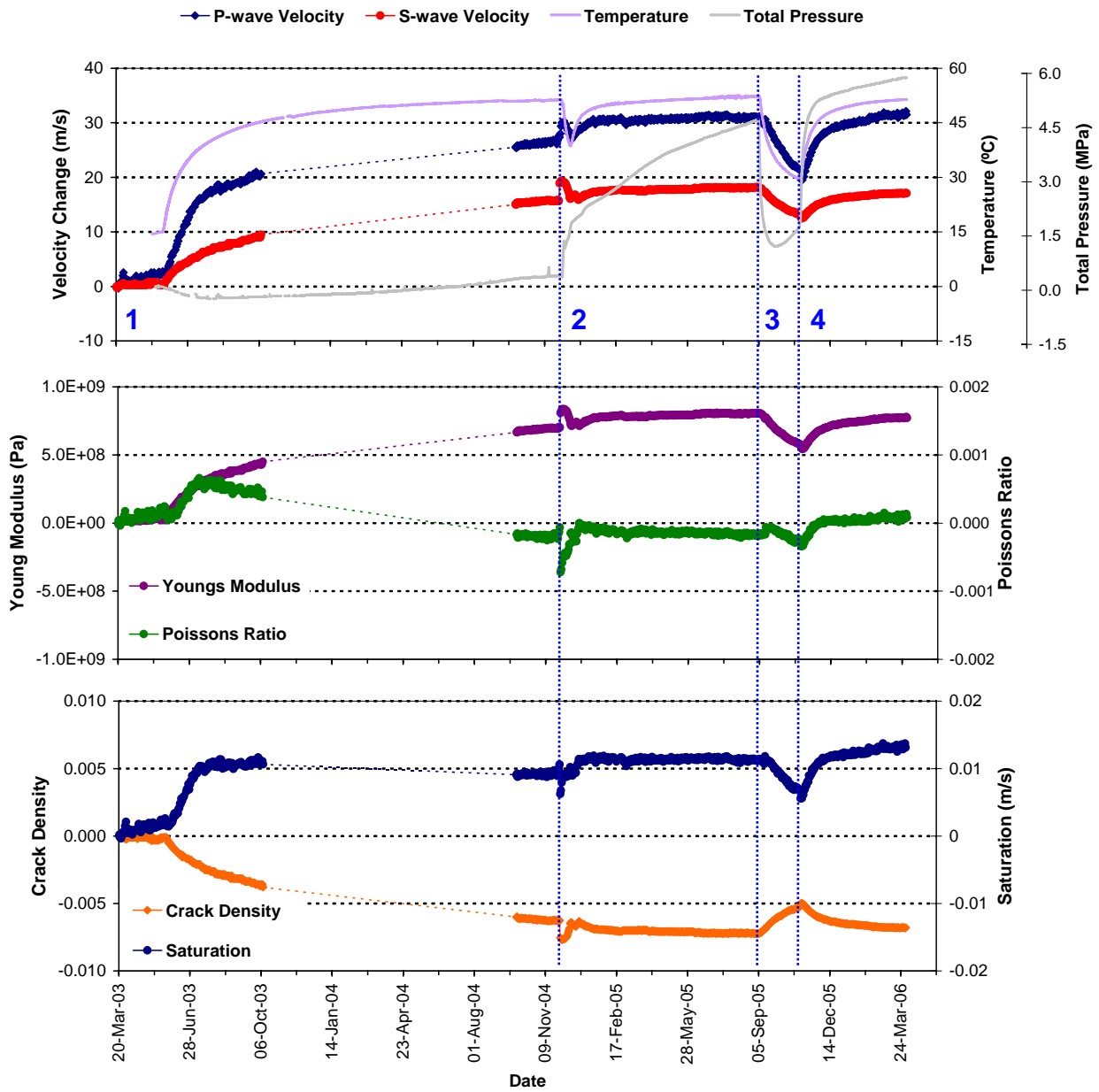
Figure 5-3: *Average P- and S-wave velocity change for raypaths on category 'S3' together with temperature (TR6045) and total pressure (PB616) (top), Young's Modulus and Poison's Ratio change (middle), and Crack Density and Saturation change (bottom).*
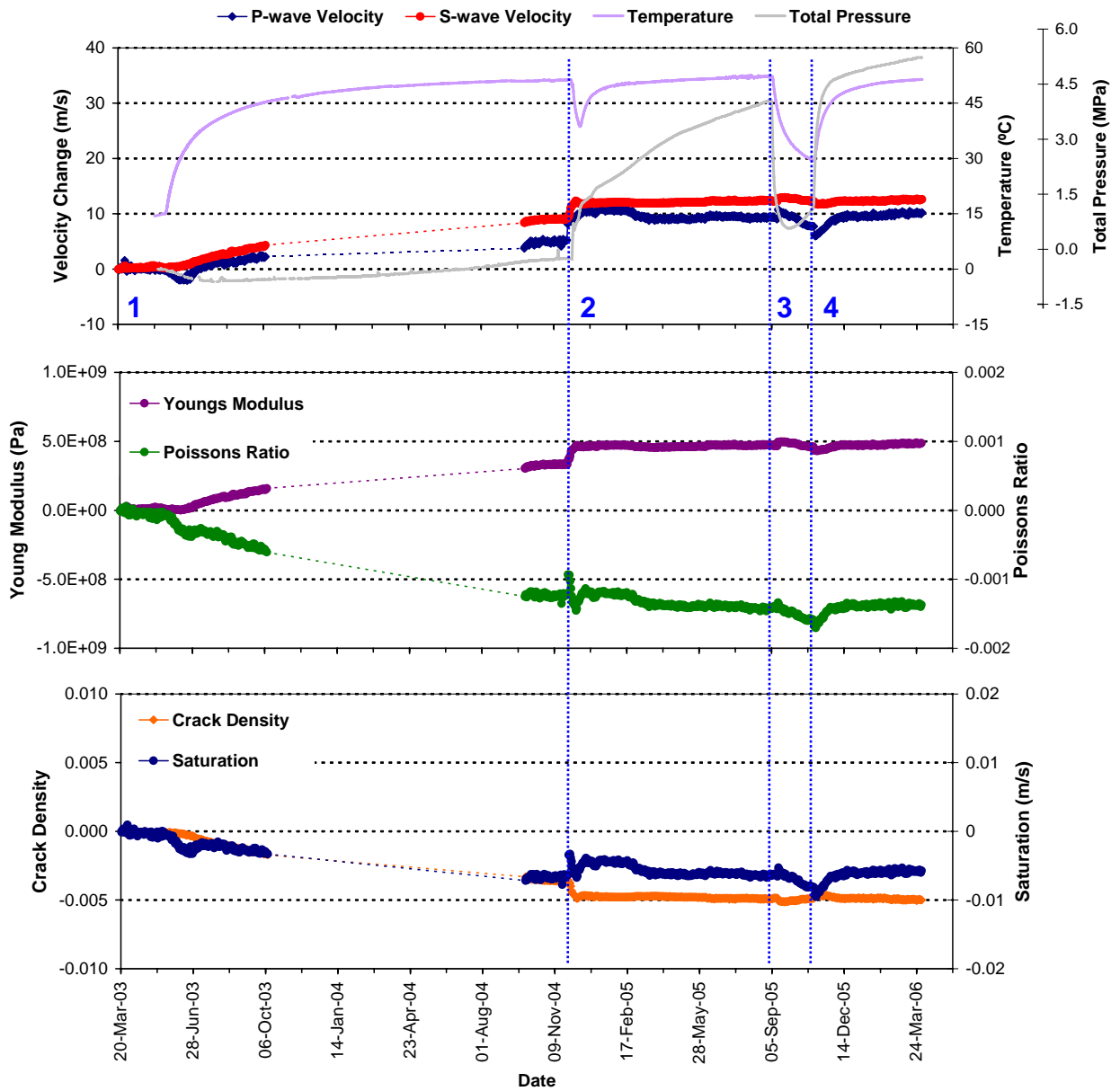
Figure 5-4: *Average P- and S-wave velocity change for raypaths on category 'C1' together with temperature (TR6045) and total pressure (PB616) (top), Young's Modulus and Poison's Ratio change (middle), and Crack Density and Saturation change (bottom).*
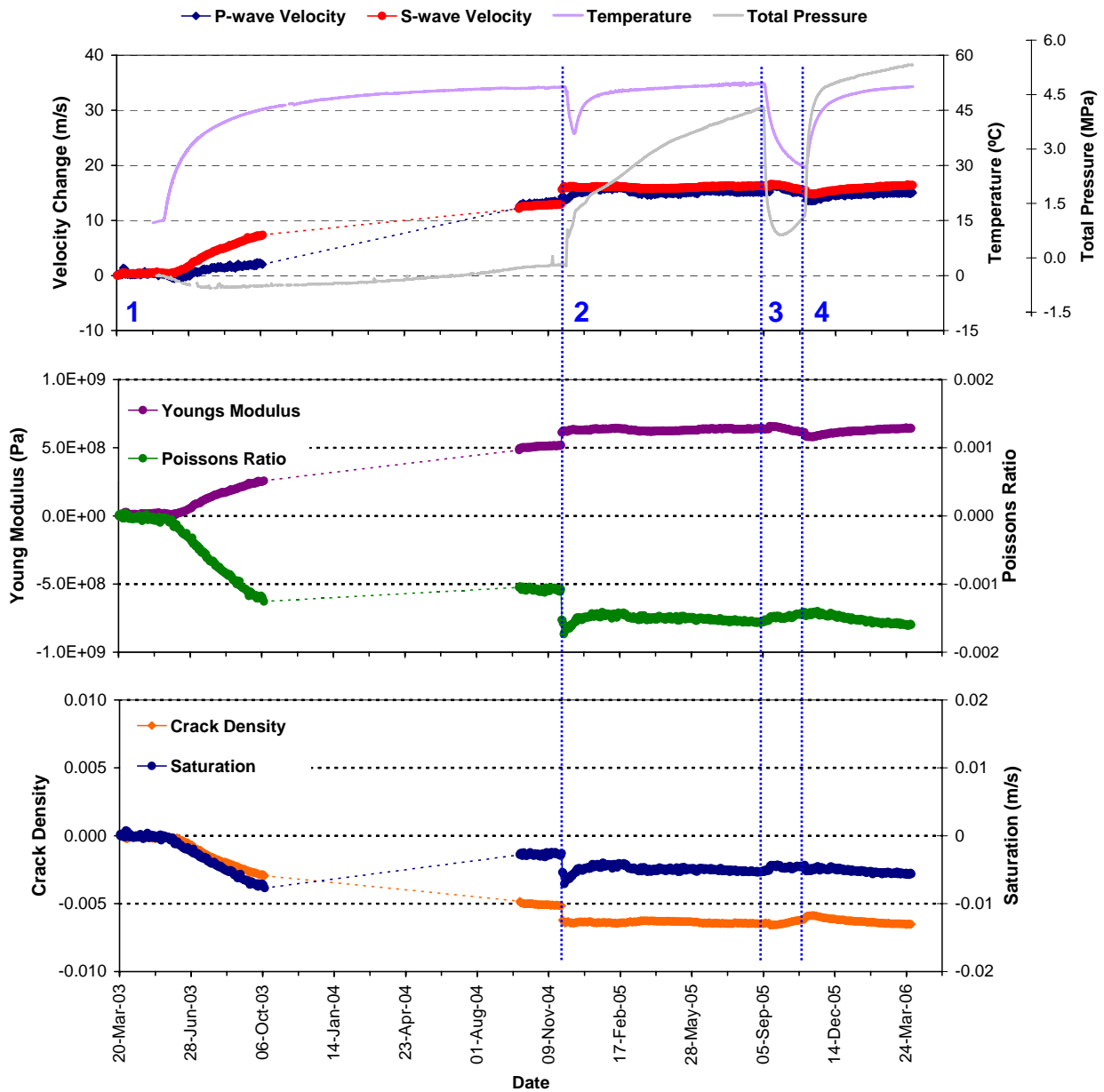
Figure 5-5: *Average P- and S-wave velocity change for raypaths on category 'C2' together with temperature (TR6045) and total pressure (PB616) (top), Young's Modulus and Poison's Ratio change (middle), and Crack Density and Saturation change (bottom).*
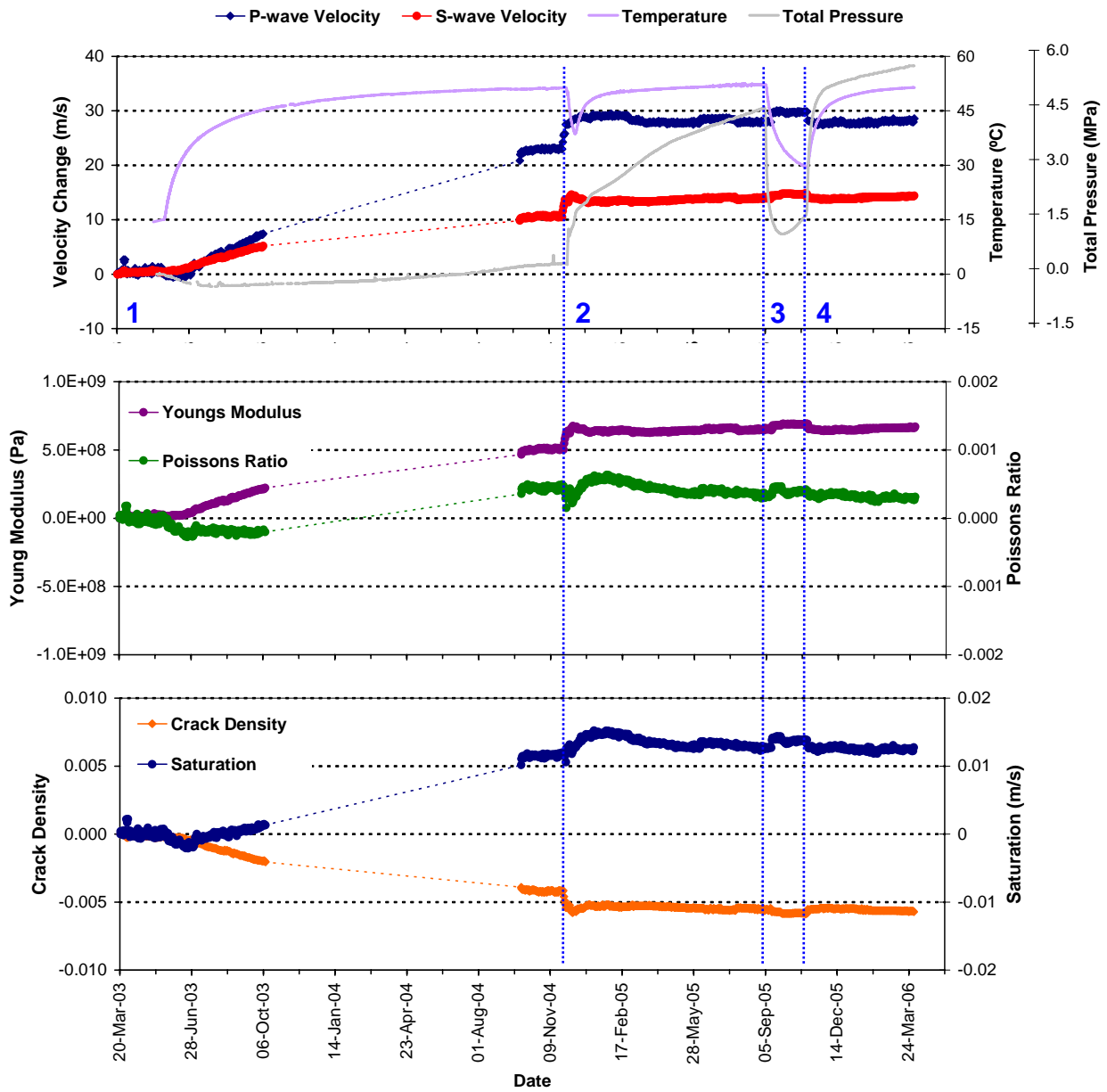
Figure 5-6: *Average P- and S-wave velocity change for raypaths on category 'Far' together with temperature (TR6045) and total pressure (PB616) (top), Young's Modulus and Poison's Ratio change (middle), and Crack Density and Saturation change (bottom).*
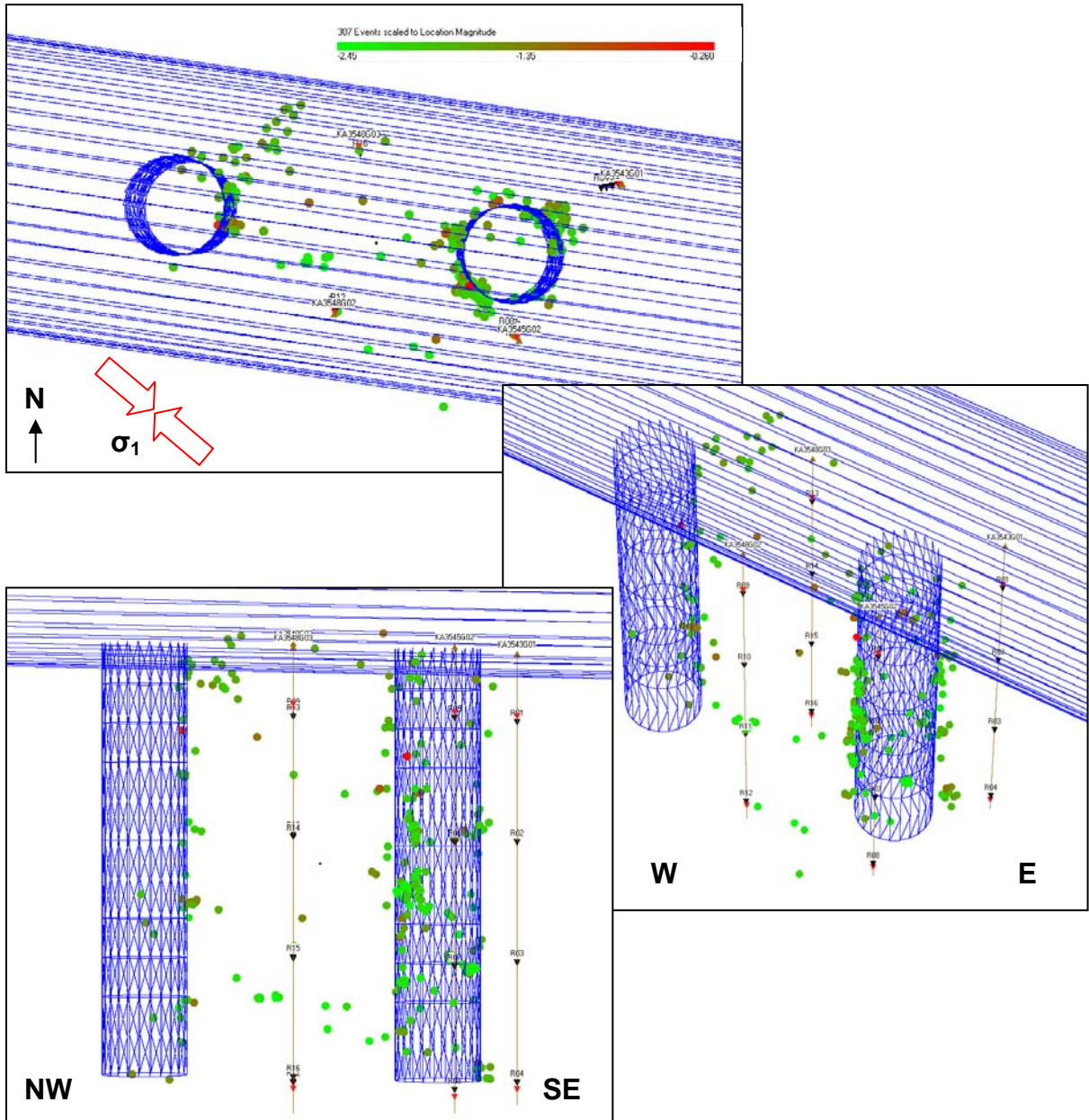
Figure 5-7: *Projections of all AEs located during the heating phase. Events are scaled to location magnitude.*
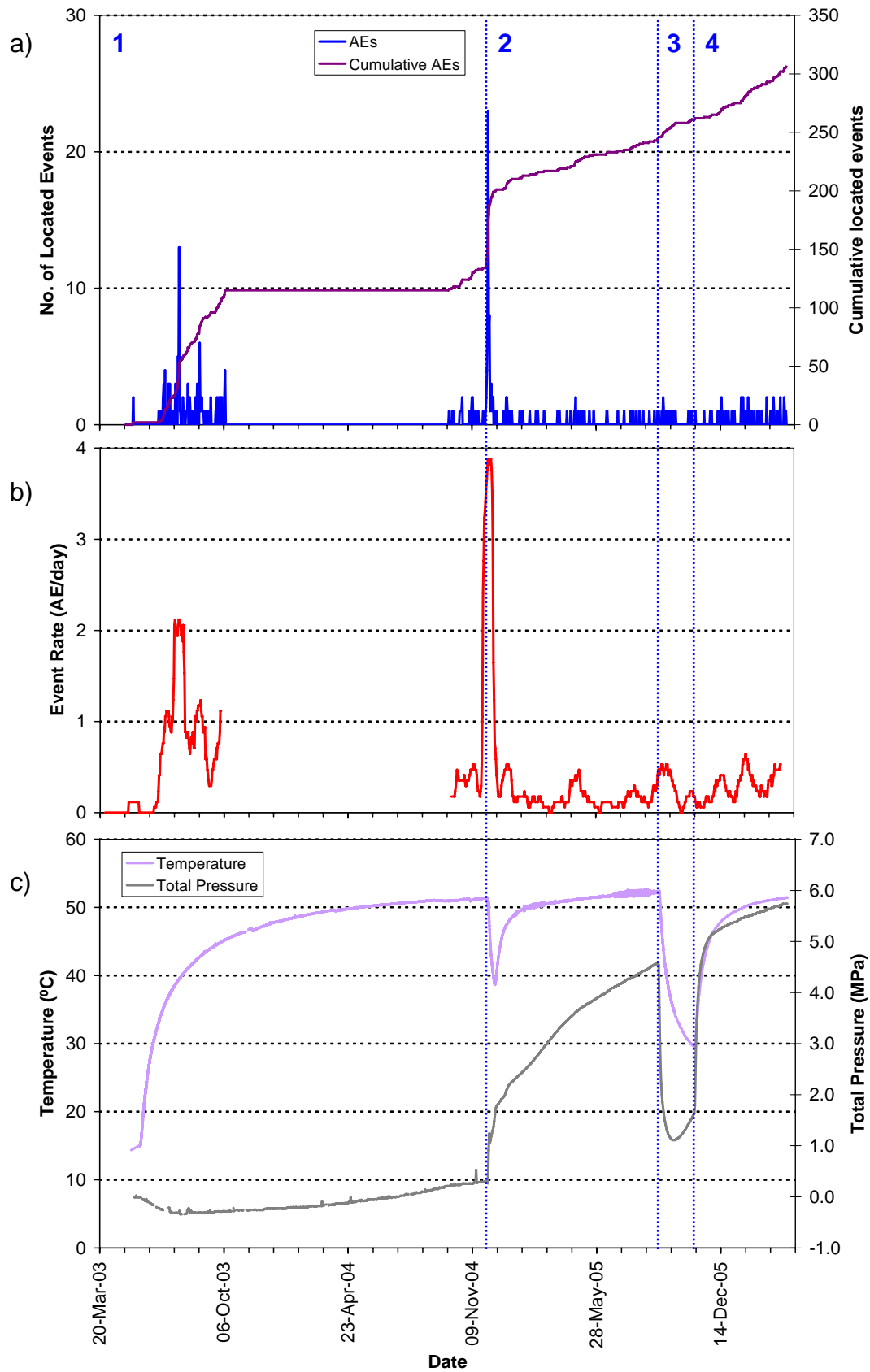
Figure 5-8: *(a) Number and cumulative number of located events from the start of monitoring, (b) average number of AE events per day (averaged over 17 days) and (c) temperature (TR6045) and pressure (PB616) measurements in deposition hole DA3545G01.*

PERIOD 1
25th May 2003 to
31st October 2004

FAR

Rock becomes
stiffer and crack
density reduces.
Saturation
increases.

**Temperature
increase**

**Pressure
constant**

S1

C2

Region
desaturates and
has slight reduction
in crack density.

C1

Through
canister

S3
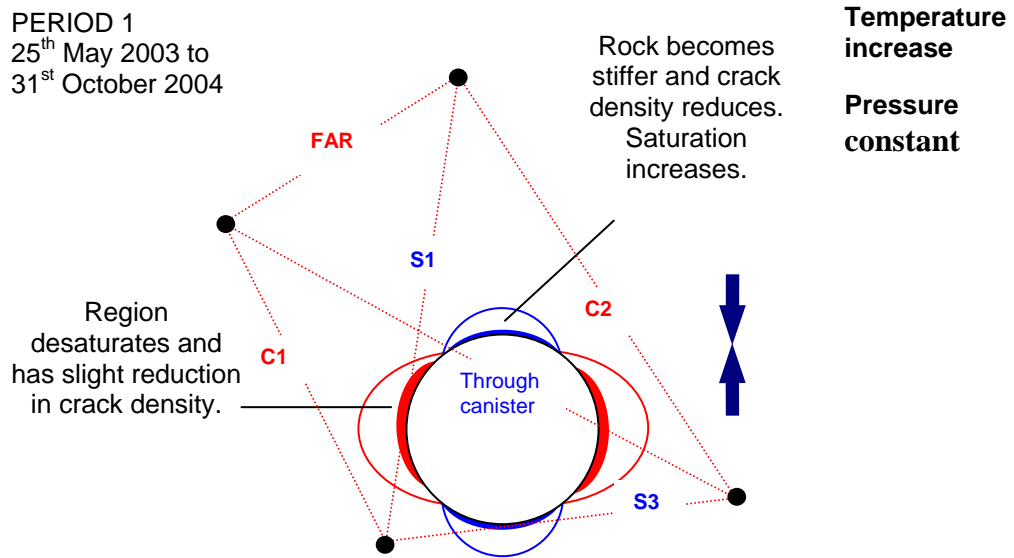
*Figure 5-9: Schematic diagram of the deposition hole and explanation of changes
experienced during Period 1.*

PERIOD 2
1st November 2004 to
4th September 2004

FAR

Decrease in
crack density
and increase in
stiffness

**Temperature
decrease, then
increase**

**Pressure
increase**

S1

C2

Decrease in crack
density and
increase in
stiffness

C1

Through
canister

S3
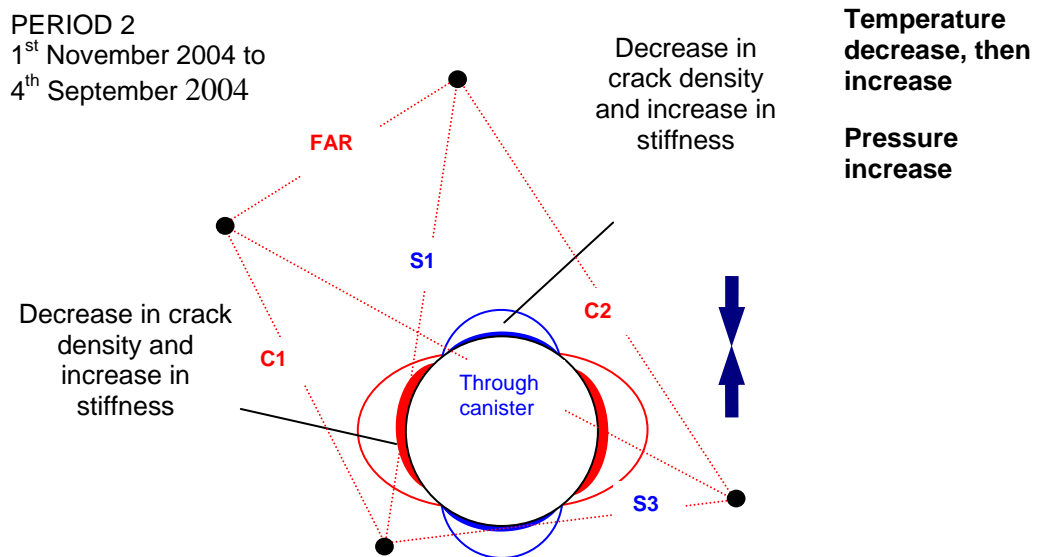
*Figure 5-10: Schematic diagram of the deposition hole and explanation of changes
experienced during Period 2.*

PERIOD 3
5th September 2005 to
2nd November 2005

FAR

Decrease in
stiffness of this
region. Crack
density
increases.

**Temperature
decrease**

**Pressure
decrease**

S1

C2

Increase in
stiffness of this
region. Crack
density reduces.

C1

Through
canister

S3
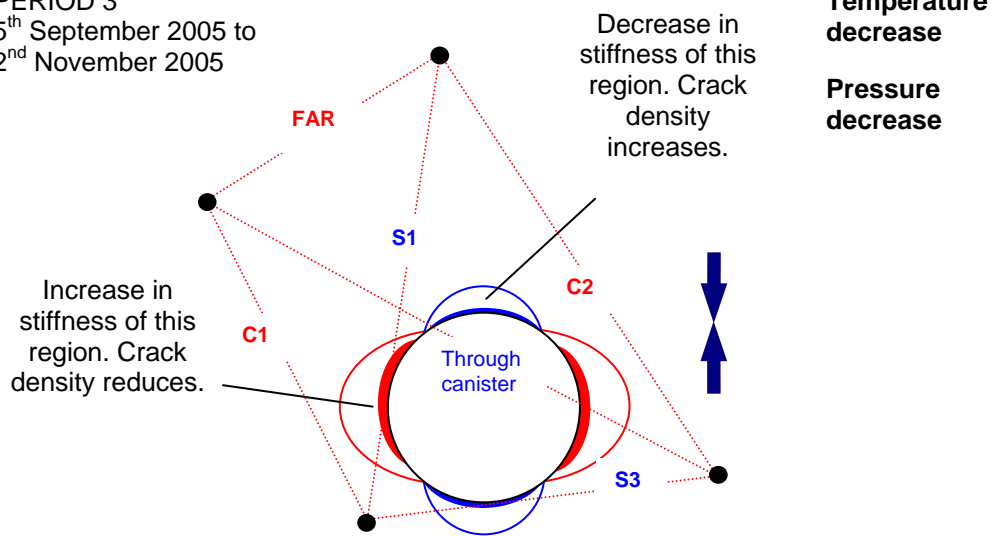
Figure 5-11: Schematic diagram of the deposition hole and explanation of changes experienced during Period 3.

PERIOD 4
3rd November 2005 to
31st December 2006

FAR

Decrease in
crack density
and increase in
stiffness.

**Temperature
increase**

**Pressure
increase**

S1

C2

Decrease in crack
density and
increase in
stiffness.

C1

Through
canister

S3
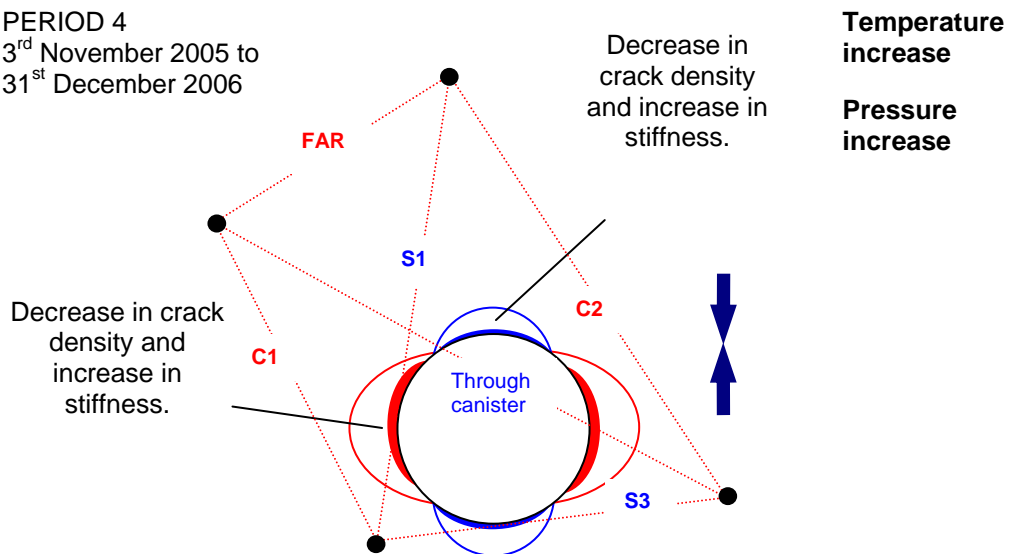
Figure 5-12: Schematic diagram of the deposition hole and explanation of changes experienced during Period 4.

6   Results Summary and Conclusions

6.1   Overview

- This report describes results from acoustic emission (AE) and ultrasonic monitoring around a canister deposition hole (DA3545G01) in the Prototype Repository Experiment at SKB's Hard Rock Laboratory (HRL), Sweden. The monitoring aims to examine changes in the rock mass caused by an experimental repository environment, in particular due to thermal stresses induced from canister heating and pore pressures induced from tunnel sealing. Monitoring of this volume has previously been performed during excavation [*Pettitt et al.*, 1999], and during stages of canister heating and tunnel pressurisation [*Haycox and Pettitt,* 2005a,b]. This report relates to the period between 1st October 2005 and 31st March 2006, and is the second of an ongoing 6-monthly processing and interpretation of the results for the experiment.

- The Prototype Repository Experiment has been designed to simulate a disposal tunnel in a real deep repository for disposal of high-level radioactive waste. Two techniques are utilised here to investigate the processes occurring within the rock mass around the deposition hole. AE monitoring is a 'passive' technique similar to earthquake monitoring but on a much smaller distance scale (source dimensions of millimetres). AEs occur on fractures in the rock when they are created or when they move. Ultrasonic surveys are also used to 'actively' examine the rock. In this case an array of transmitters sends signals to an array of receivers. Amplitude and velocity changes on the ray paths can then be used to examine changes in the rock's properties (Young's modulus, Poisson's ratio, Crack density and Saturation).

- AE and Ultrasonic monitoring has previously been conducted at the Prototype Repository during excavation of two deposition holes in Section II of the tunnel and when simulated canisters, installed in the deposition holes, were first heated and the tunnel pressurised. A summary of the key results from these monitoring periods is provided in Section 3. Monitoring is now continuing in 6-monthly reporting periods using a permanent ultrasonic array, with transducers installed into instrumentation boreholes in June 2002, before the tunnel was sealed. In April 2003 heaters in the simulated waste canisters were switched on causing temperatures to rapidly increase in the rock mass up to approximately 50°C at the rock wall. In November 2004 water drainage from the sealed Prototype tunnel was stopped causing a rapid increase in fluid pressures in the deposition hole. An exponential decrease in temperature and pressure occurred when heaters were switched off and drainage to the tunnel re-opened in September 2005.

- This monitoring period relates to the six-months starting 1st October 2005. Initially, from September 2005, temperature around the deposition hole is observed to decrease. On 3rd November 2005, the temperature is observed to increase again. Pressure is observed to increase from 1st November 2005. After an initial rapid increase, measured pressure and temperature increase at a constant rate for the rest of the reporting period.

6.2   Ultrasonic Surveys

- Velocity changes are measured between transmitter-receiver pairs on the daily ultrasonic surveys using a cross-correlation technique that allows a velocity resolution of $\pm 2 m.s^{-1}$. Average P- and S-wave velocity reduces over the first month at a consistent rate, P-wave velocity decreasing slightly faster than S-wave velocity. Between 2nd and 3rd November 2005 there is a drop in P-wave velocity of $1.5 m.s^{-1}$ and S-wave velocity of $0.5 m.s^{-1}$. After the sudden drop, both P- and S-waves show increases in velocity, such that by the end of the reporting period average velocity is slightly faster than at the start. The sudden drop is a significant change, given that the average is determined from velocity measured on many raypaths. A decrease in Young's Modulus occurs which indicates a reduction in stiffness of the rock. This short term change is likely to be a sudden reaction of the rock mass to the increase in pressure, perhaps caused by a general opening of microcracks caused by increased pore pressures. The long term trend is to then close these microcracks from increased thermal stresses. Further work is required to de-couple the response of temperature and pressure change in the velocity and amplitude results. The sudden change in pressure is not accompanied by an increase in the rate of AE or trigger activity indicating no further damage is occurring to the rock.

- A variation is also observed in the average amplitude measurements during the time period. For the first month, P- and S-wave amplitudes decrease at a relatively constant rate. A minimum is reached on 6th November 2005. After this date amplitudes rapidly increase, closely correlating with temperature and pressure measured around the deposition hole. By the end of the reporting period, the P and S-wave amplitudes are slightly higher than at the start. The S-wave is shown to be slightly more responsive than P-wave.

- Rock parameters (Young's Modulus, Poisson's Ratio, Crack Density and Saturation) have been calculated from the average measured velocities for the ray path categories. Young's Modulus decreases when the rock is de-pressurised and temperature is reduced. Crack density increases during the first month of the monitoring period, when cooling and de-pressurisation led to microcracks reopening. The rock parameters have been compared between ray path positions with respect the deposition hole geometry. Least affected by the pressure and temperature variations is the 'Far' raypath category. Ray paths that skim close to the deposition hole surface in the 'S3' category show the largest reduction. These raypaths pass through a zone of tensile or low compressive stresses. Microfractures in this region are most responsive to changes in thermal stress due to being under low stress. When pressure and temperature increase, the crack density is observed to reduce, particularly on the 'S3' raypath category.

- The initial reduction in the stiffness of rock around the deposition hole, and increase in crack density, is a continuation of conditions that existed at the end of the previous monitoring period. The response is interpreted as an opening of existing microfractures and pore spaces in the region of low-compressive or tensile stresses. This is a result of a cooling of the rock and reduction in pressure from the deposition hole interior, returning the rock to a state prior to heating when microfractures were relatively more open. When temperature and pressure increase, the associated increase in stiffness and decrease in crack density can be interpreted as the closing of existing microfractures and pore spaces. Existing microcracks in the low-compressive or tensile region were initially unloaded immediately after excavation. Consequently they are more reactive to stress changes than in the compressive region where stresses act to pre-close the microcracks. Large changes were also observed on this category when heating commenced.

6.3　Acoustic Emissions

- Fifty AEs have been located with high confidence from 100 triggered events recorded during this period. Two distinct peaks in activity are recognised with 18 triggers on 31st October 2005 and 10 triggers on 9th January 2006. An average number of 0.27 events are located per day, with no more than 2 AEs located on a single day. This is an increase on the previous six months (0.21 event per day), but lower than six months before (0.32 events per day). However, when compared to the high level of activity observed during excavation, in which up to 20 events per hour were recorded, this represents a very low level. The majority of the events locate in the immediate vicinity of deposition hole DA3545G01. Three events also locate close to the neighbouring deposition hole DA3551G01. A cluster of 39 events is situated on the SE side of deposition hole DA3545G01 at a depth of 455.1m, in the low-compressive, or tensile stress, region. In previous monitoring periods, the majority of events were distributed in the NE and SW quadrants which coincide with regions of increased compressive stress as imaged during excavation and initial stages of heating [*Pettitt et al.*, 2000; *Pettitt et al.*, 2002]. Smaller clusters were observed in orthogonal regions of low-compressive or tensile stress. The events observed during this reporting period are therefore consistent with these previous results with events locating in regions of previous activity. The events are therefore interpreted as a continuation of activity in the previously imaged damage zone and, similar to during excavation and initial heating, are created either by movement on pre-existing microcracks, or as a result of extension or formation of new microcracks in the existing damaged region.

- The frequency of located events has generally been low compared to when temperature first increased in 2003 and when the rapid change in pressure occurred in December 2004. A low number of AEs suggests the rock mass has stabilised. Despite a rapid increase in temperature during the most recent monitoring period, the rate of AEs is still low and consistent with previous monitoring. The pressure measured in the deposition hole increased to over 4.5MPa on one instrument by September 2005. This lead to a confining pressure being placed on the rock around the deposition hole and could explained the cessation in AEs as movement on macrofractures and microcracks is inhibited. This is a response observed in laboratory rock tests [*Pettitt and Haycox*, 2004], and in the Tunnel Sealing Experiment (TSX) at AECL's Underground Research Laboratory (URL) [*Baker and Young*, 2003].

- Pressure decreased rapidly in September 2005 when additional drainage to the tunnel is opened. Pressure increases rapidly again approximately 2 months later. This appears to have no significant affect on the number, or distribution of AEs around the deposition hole. This differs to the results in December 2004 when a rapid pressure *increase* caused 32 events to locate in clusters over the course of two days. The events recorded then were interpreted as stress changes in the rock as it responds to the sudden pressure change. This induces small scale movement on pre-existing microcracks, or induces new microfractures in weaker volumes of the rock. Although a cluster of events has been located over the last 6 months, changes in pressure and temperature have not caused a sufficient redistribution of stresses to initiate further microfracturing.

References

Baker, C. and R.P. Young. 2002. Acoustic emission and ultrasonic monitoring around the TSX tunnel clay and concrete bulkheads between October 2001 and October 2002. Ontario Power Generation, Nuclear Waste Management Division Report.

Goudarzi, R. and L-E. Johannesson, Sensor Data Report (Period: 010917-050601). Prototype Repository. Report No: 13, International Progress Report IPR-05-28, Äspö Hard Rock Laboratory, Swedish Nuclear Fuel and Waste Management Company, Sweden, 2006.

Goudarzi, R., 2005. Pers. Comm.

Goudarzi, R., 2006. Pers. Comm.

Haycox, J.R. and W.S. Pettitt, Acoustic Emission and Ultrasonic Monitoring During the Heating of Deposition hole DA3545G01 in the Prototype Repository to March 2005, International Progress Report IPR-05-30, Äspö Hard Rock Laboratory, Swedish Nuclear Fuel and Waste Management Company, Sweden, 2005a.

Haycox, J.R. and W.S. Pettitt, Acoustic Emission and Ultrasonic Monitoring Results from Deposition Hole DA3545G01 in the Prototype Repository between April 2005 and September 2005, International Progress Report IPR-05-31, Äspö Hard Rock Laboratory, Swedish Nuclear Fuel and Waste Management Company, Sweden, 2005b.

Johannesson, L-E., 2005. Pers. comm.

Johannesson, L-E., 2006. Pers. comm.

Maxwell, S.C., and R.P. Young, A controlled in-situ investigation of the relationship between stress, velocity and induced seismicity, Geophys. Res. Lett., 22, 1049-1052, 1995.

Patel, S., L.-O. Dahlstrom, and L. Stenberg, Characterisation of the Rock Mass in the Prototype Repository at Äspö HRL Stage 1, Äspö Hard Rock Laboratory Progress Report HRL-97-24, Swedish Nuclear Fuel and Waste Management Company, Sweden, 1997.

Pettitt, W.S., C. Baker, and R.P. Young, Acoustic emission and ultrasonic monitoring during the excavation of deposition holes in the Prototype Repository, International Progress Report IPR-01-01, Äspö Hard Rock Laboratory, Swedish Nuclear Fuel and Waste Management Company, Sweden, 1999.

Pettitt, W.S., C. Baker, and R.P. Young, Analysis of the in-situ principal stress field at the HRL using acoustic emission data, International Progress Report IPR-01-09, Äspö Hard Rock Laboratory, Swedish Nuclear Fuel and Waste Management Company, Sweden, 2000.

Pettitt, W.S., C. Baker, R.P. Young, L. Dahlstrom, and G. Ramqvist, The assessment of Damage Around Critical Engineering Structures Using Induced Seismicity and Ultrasonic Techniques, Pure and Applied Geophysics, **159**, 179-195, 2002.

Pettitt, W.S., Baker, C., Collins, D.S., and R.P. Young, 2005. InSite Seismic Processor – User Operations Manual Version 2.13. Applied Seismology Consultants Ltd., Shrewsbury, UK.

Pettitt, W.S. and J.R. Haycox, Acoustic emission observations of rock fracture under true-triaxial stress. In SAFETI Year 2 Progress Report, University of Liverpool, UK, 2004.

SKB, Äspö Hard Rock Laboratory: Current Research Projects 1998, Swedish Nuclear Fuel and Waste Management Company, Sweden, 1999.

Telford, W.M., Geldart, L.P., and Sheriff, R.E., Applied Geophysics: Second Edition, Cambridge University Press, 1990.

Young, R.P. and W.S. Pettitt, Investigating the stability of engineered structures using acoustic validation of numerical models, in Geotechnical Special Publication No 102, edited by J.F. Labuz, S.D. Glaser, and E. Dawson, pp. 1-15, ASCE, USA, 2000.

Zimmerman, R.W and M.S. King, Propogation of acoustic waves through cracked rock, 20th Symposium on Rock Mechanics, Rapid City, SD, 1985.

Appendix I   Methodology

Data Acquisition

The ultrasonic array consists of twenty-four ultrasonic transducers configured as eight transmitters and sixteen receivers installed into four instrumentation boreholes. The transducers are fixed into the boreholes using specially designed frames (Figure 6-1) – two transmitters and four receivers per frame. The boreholes are vertical, 76mm in diameter and approximately 10 meters in length distributed around each deposition hole volume. The array has been designed so as to provide good coverage for AE locations and to provide 'skimming' ray paths that pass within a few centimetres of the deposition-hole void so as to sample the rock immediately adjacent to the deposition-hole wall. The layout of the instrumentation boreholes is shown in Figure 6-2 and described further in Table 6-1. Each of the ultrasonic transducers has a hemispherical brass cap fixed over its active face and is then spring-loaded against the borehole surface so as to obtain good coupling to the rock mass. The boreholes have then been filled with a slightly expansive grout so as to permanently fix the transducers in place, reduce the likelihood of damage to the transducers and to remove the borehole voids.
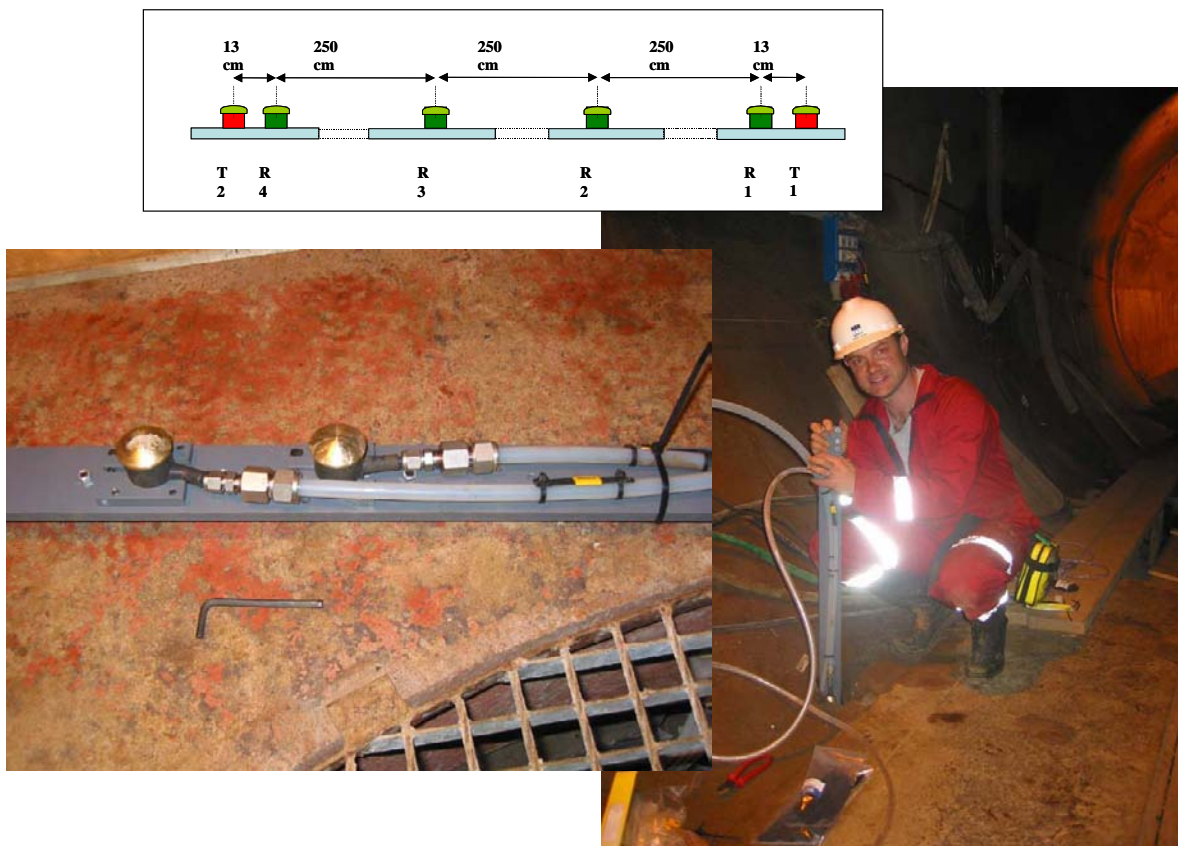

Figure 6-1: *Top: Schematic diagram of the locations of all transducers on a single frame. Left: Photo of a section of the transducer assembly. Right: The transducer assembly during installation.*

The piezoelectric transducers operate by converting a transient elastic wave into an electric signal or visa versa. The monitoring system is then operated in one of two modes. The first is used to passively monitor AE activity preferentially within the array volume. AEs release elastic energy in the same way as 'earthquakes' but over a very small scale. At these frequencies AEs have a moment magnitude (M_w) of approximately -6. They occur either during the creation process of new fractures within the medium, or on pre-existing fractures due to small scale movements. Each receiver has a frequency response of approximately 35-350kHz and contains a 40dB pre-amplifier. This minimises a reduction in signal-to-noise between the sensors and the acquisition system. The sensors have a vulcanised surround and a high pressure reinforced cable to protect them from water infiltration. In addition, polyamide tubes and *Swagelok* connectors have been fitted to the cables to reduce the likelihood of breakage.

Figure 6-3 shows a schematic diagram of the acquisition system used. Cables from each transducer pass through the pillar between the PRT and the G-tunnel. Data acquisition uses a Hyperion Ultrasonic System controlled by a PC, set up within a cabin provided by SKB. This has 16 receiving channels and 8 transmitting channels. An AE is recorded when the amplitude of the signal on a specified number of channels exceeds a trigger threshold within a time window of 5ms. The system then records the full-waveform signals from all 16 transducers. In this case a trigger threshold of 50mV on three channels was used. This allows the system to have sufficient sensitivity to record high quality data without recording an abundance of activity that cannot be processed due to very small signal to noise on only a few channels. The captured signals are digitised with a sampling interval of 1μs and a total length of 4096 data points. In general, low noise levels were observed (<2mV) giving high signal to noise and good quality data. AE monitoring is set to switch off during daytime working hours (6am-8pm) so as to minimise the amount of noise recorded from human activity.

A second operating mode actively acquires ultrasonic waveforms by scanning across the volume. This allows measurements of P- and S-wave velocities and signal amplitudes over a possible 128 different ray paths. By repeating these ultrasonic surveys at increments in time, a temporal analysis is obtained for the variation in medium properties. Ultrasonic surveys are conducted daily at 1am in order to measure changes in P- and S-wave signals. At that time of night, no human activity will cause noise that can interfere with the signals received. A Panametrics signal generator is used to produce a high frequency electric spike. This is sent to each of the 8 transmitters in turn. The signal emitted from each transmitter is recorded over the 16 receivers in a similar fashion to that described above. An external trigger pulse from the signal generator is used to trigger the acquisition system and identifies the transmission start time to an accuracy of one sample point. In order to decrease random noise the signal from each transmitter is stacked 100 times.

Table 6-1: Boreholes used for AE monitoring of deposition hole DA3545G01.

SKB Borehole designation	ASC Borehole reference	Transducer Numbers
KA3543G01	1	T1, T2, R1-R4
KA3545G02	2	T3, T4, R5-R8
KA3548G03	3	T5, T6, R9-R12
KA3548G02	4	T7, T8, R13-R16
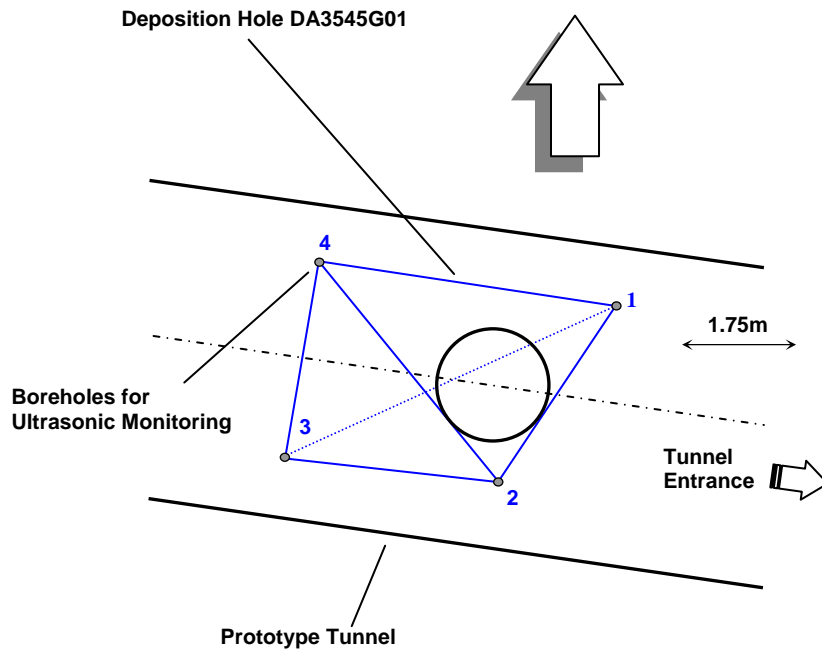
Figure 6-2: *Plan view of the array geometry for Deposition Hole DA3545G01 during heating in the Prototype Tunnel. The blue solid lines represent direct raypaths between sondes illustrating their 'skimming' nature. The blue dashed line represents a raypath that travels through the deposition hole.*
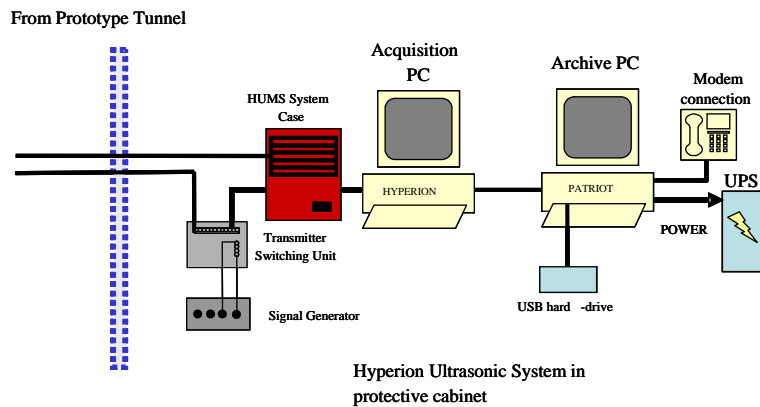
Figure 6-3: *Schematic diagram of the hardware used for the heating stage in the Prototype Repository. The ultrasonic pulse generator sends a signal to each transmitter and the resulting signal is recorded on each receiver. The receivers are also used to listen for AE activity. The archive PC is required to make a copy of the data for backup purposes.*

Processing Procedure

Overview

ASC's InSite Seismic Processor has been used to automatically process both the AE and ultrasonic survey data. Appendix 1A and Appendix 1B give the processing parameters used. *Pettitt et al.*[2005] provides a detailed description of this software.

Ultrasonic Data Procedure

The ultrasonic survey full-waveform data was initially stored with the AE data. This was automatically sorted and the survey data extracted to a separate processing project. A 'reference' survey from the previous monitoring period was used, and imported into the project. The P- and S-wave arrivals were manually picked during the previous monitoring period. Knowing the transmitter and receiver locations, the ultrasonic velocity for each ray path was calculated with an estimated uncertainty of ±30m.s^{-1} (±3 data points). A cross-correlation procedure was then used to automatically process subsequent surveys. This technique cross-correlates P- and S-wave arrivals from a transmitter-receiver pair with arrivals recorded on the same transmitter-receiver pair on the reference survey. This results in high-precision measurements of P- and S-wave velocity change with estimated uncertainties of ±2m.s^{-1} between surveys. Note that when the transmitter and receiver are on the same borehole, the raypath is not used due to the introduction of transmission effects from the instrumentation borehole, grout and transducer frames.

The main reason for the reduction of uncertainty when using the cross-correlation procedure is the dependency of manual picking on the user's judgement of the point of arrival. This can usually be quite indiscriminate because of random noise superimposed on the first few data points of the first break. Additionally, the procedure is run automatically without any loss of precision resulting in efficient waveform processing. The cross-correlation procedure then allows for a high-resolution analysis to be performed and hence small changes in velocity to be observed. This is extremely important when changes in rock properties occur over only a small section (5%) of the ray path.

Figure 6-4 gives example waveforms recorded from one of the transmitters during this reporting period. Each waveform is first automatically picked to obtain an estimate of the P-wave or S-wave arrival. A window is then automatically defined around the arrival and a bell function is applied, centred on the automatic pick. The data at the ends of the window then have a much smaller effect on the cross-correlation. The windowed data is then cross-correlated [*Telford et al.*, 1990] with a similar window constructed around the arrival on the reference survey. The change in arrival time is then converted to a change in velocity knowing the manually-picked arrival time for the reference survey. Waveforms that do not provide automatic picks are not cross-correlated. This gives an automatic discrimination of signals that have very poor signal to noise ratios and could give spurious cross-correlation results from poor discrimination of the first arrival. During the automatic processing an arrival amplitude is also calculated from within a processing window defined by a minimum and maximum transmission velocity. This provides a robust measure of arrival amplitudes between surveys.
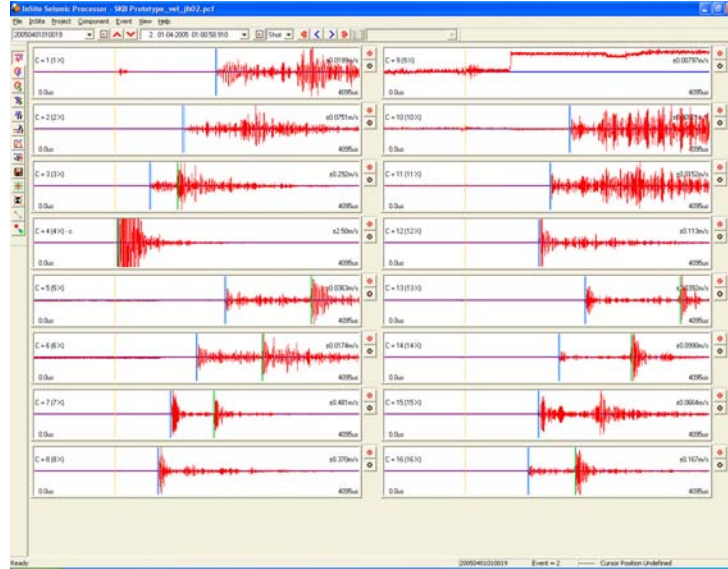
Figure 6-4: Waveforms recorded from one transmitter on the array of sixteen receivers. The gold markers indicate the transmission time. The blue and green markers indicate picked P- and S-wave arrivals respectively.

When calculating average velocities and amplitudes, raypaths passing through the deposition hole are removed due to the uncertain transmission paths produced by the wave travelling in the rock around the deposition hole and through the bentonite, fluid and canister fill. Therefore the majority of raypaths between boreholes 1 and 3 (transmitters 1, 2, 5, 6 and receivers 1, 2, 3, 4) are not used in the analysis. An exception is made for the deepest raypaths that pass under the deposition hole entirely through rock Raypaths that pass through the deposition hole are still processed and an analysis of the results can be found in Section 5.

The dynamic Young's modulus E, and dynamic Poisson's Ratio, v, can be calculated from the velocity measurements using Equation 1 and Equation 2

$$E = \rho V_S^{\,2}\left(\frac{3V_P^{\,2} - 4V_S^{\,2}}{V_P^{\,2} - V_S^{\,2}}\right)$$

Equation 1

$$v = \frac{V_P^{\,2} - 2V_S^{\,2}}{2\left(V_P^{\,2} - V_S^{\,2}\right)}$$

Equation 2

V_P and V_S values are also used to model for crack density (c) and saturation (s) in the rock mass using the method of *Zimmerman and King*[1985]. The crack density parameter is defined by the number of cracks (penny-shaped) per unit volume multiplied by the mean value of the cube of the crack radius (Equation 3). This method assumes the elastic modulus E and v in the damaged material normalized to the undisturbed material, decrease exponentially with crack density. Also assumed are the shear modulus (μ) is unaffected by s, and the bulk modulus (k) increases linearly with s, equalling that of uncracked rock when $s=1$. Equation 4 shows the calculation used to determine saturation.

$$c = \frac{9}{16} \ln\left(\frac{2\mu}{E_0 - 2\mu v_0} \right)$$

Equation 3

$$s = \frac{k(c,s) - k(c,0)}{k_0 - k(c,0)}$$

Equation 4

The calculations require an estimation of the completely undisturbed rock (i.e. an unsaturated, uncracked, intact rock mass). This study assumes values of $V_{0P} = 6660 \text{m.s}^{-1}$, and $V_{0S} = 3840 \text{m.s}^{-1}$ for the undisturbed material taken from laboratory tests on a similar granite, summarized in *Maxwell and Young*[1995]. A value of 2650 kg m^{-3} is presented by *Pettitt et al.*[2002] for the density of the rock mass.

The calculations of Young's Modulus and Poisson's ratio from measured velocities makes an assumption of an isotropic elastic medium. Under this assumption a rock can be completely characterised by two independent constants. One case of an isotropic elastic medium is a rock with a random distribution of cracks embedded in an isotropic mineral matrix. Under the application of a hydrostatic compressive stress, the rock will stay isotropic but become stiffer (which will become characterised by increased velocity V_P, V_S and therefore increased Young's modulus). In contrast, under the application of a uniaxial compressive stress, cracks with normal's parallel or nearly parallel to the applied stress will preferentially close and the rock will take on a transversely isotropic symmetry. Under this situation P- and S-wave velocities become variable with orientation. The crack density and saturation calculations also assume an isotropic elastic medium.

It should be noted that E and v calculated in this report are dynamic measurements due to the small strains exerted on the rockmass at high frequencies from the passing ultrasonic waves. Static E and v measurements, made from uniaxial laboratory tests on rock samples, may be different from dynamic values – even if sample disturbance is minimal – due to the larger strains exerted over relatively long periods of time.

Acoustic Emission Procedure

The procedure used to process the AEs in this reporting period has been undertaken as follows:

1. Calibration surveys from the installation phase (when the deposition hole was open) have been used to optimise an automatic picking and source location algorithm and check location uncertainties. ASC's InSite seismic processing software was used for location and visualisation.

2. Where possible, P- and S-wave arrival times were measured for each AE using the automatic picking procedure.

3. AEs with ≥6 P-wave arrival times were input into a downhill-simplex location algorithm [*Pettitt et al.*, 2005]. This has the option of incorporating either a three-dimensional anisotropic velocity structure or an isotropic structure. Velocities calculated from the ultrasonic surveys were used.

4. The waveforms from all events were visually inspected to ensure they were 'real' acoustic emissions. Events were removed if they had the appearance of noise spikes (increase in amplitude is recorded on all channels at the same time) or they were the result of human noise (long period events that occur at close intervals during the day).

5. The acoustic emissions that remained had their arrivals manually picked to obtain the best possible location. Any events that located outside the expected region of activity were further checked to ensure accuracy. Experience from previous studies around deposition holes showed that large source location errors were produced if significant portions of a ray path passed through the excavated deposition hole void. This only becomes a problem for the largest AEs. AEs were reprocessed with these ray paths removed.

6. Finally, a filter was applied to remove all AEs with a location error greater than 1.0.

During the equipment installation phase, calibration shots have been undertaken to assess the sensitivity of the system to 'real' AEs and to determine the accuracy with which real events could be subsequently located by the array of sensors. A series of test 'shots' were performed on the wall of deposition hole DA3545G01 (Figure 6-5). The shots consisted of undertaking 10 'pencil lead breaks' and 10 hits with a screw-driver at 1 metre intervals down 4 lines along the deposition hole wall. The pencil-lead tests involved breaking the 0.5 mm lead from a mechanical pencil against the borehole wall. This is a 'standard' analogue for an AE as it generates a similar amount of high-frequency energy. An example of a pencil lead break test is shown in Figure 6-6. This was made at 6 metres below the tunnel surface on the deposition hole wall at a point adjacent to borehole KA3548G02. This corresponds to an AE source dimension on the millimetre scale (grain size).

The screw-driver hits provided a good amplitude signal for assessing the accuracy with which events can be located within the volume surrounded by the array. Figure 6-5 shows the results from one processed set of locations for a line of shots down the deposition hole wall. This shows that the array is able to locate events with good accuracy and consistency within an estimated uncertainty of approximately 10cm.

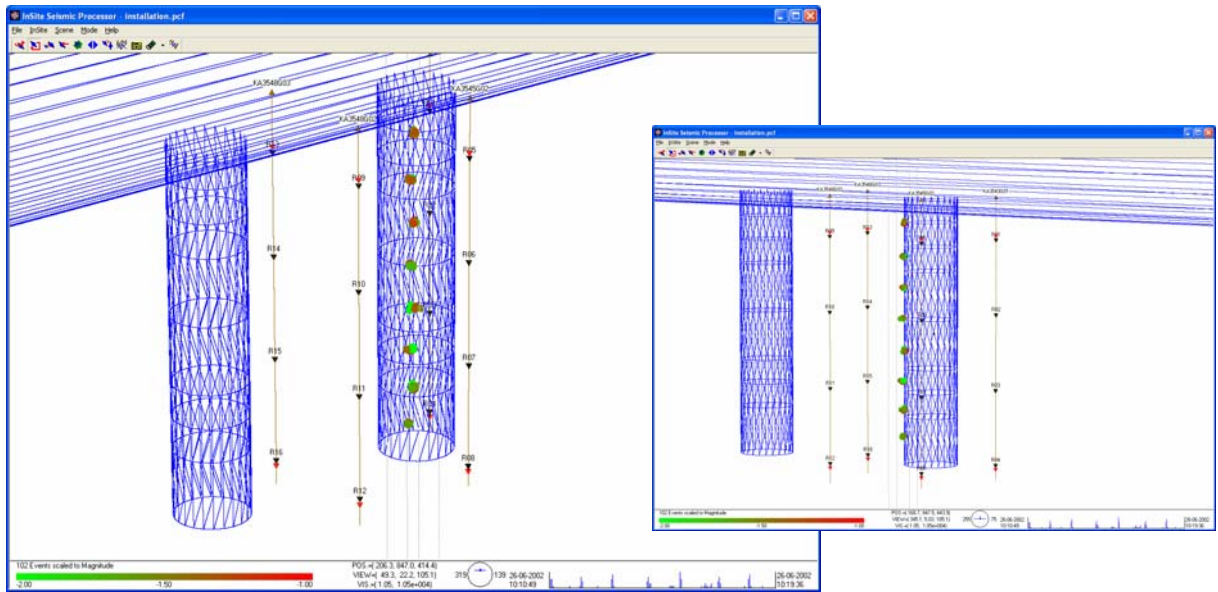**Figure 6-5:** *Locations of calibration shots obtained from a series of tests at 1 metre intervals down the wall of deposition hole DA3545G01. The two views show that these line up and are located close to the surface of the hole.*
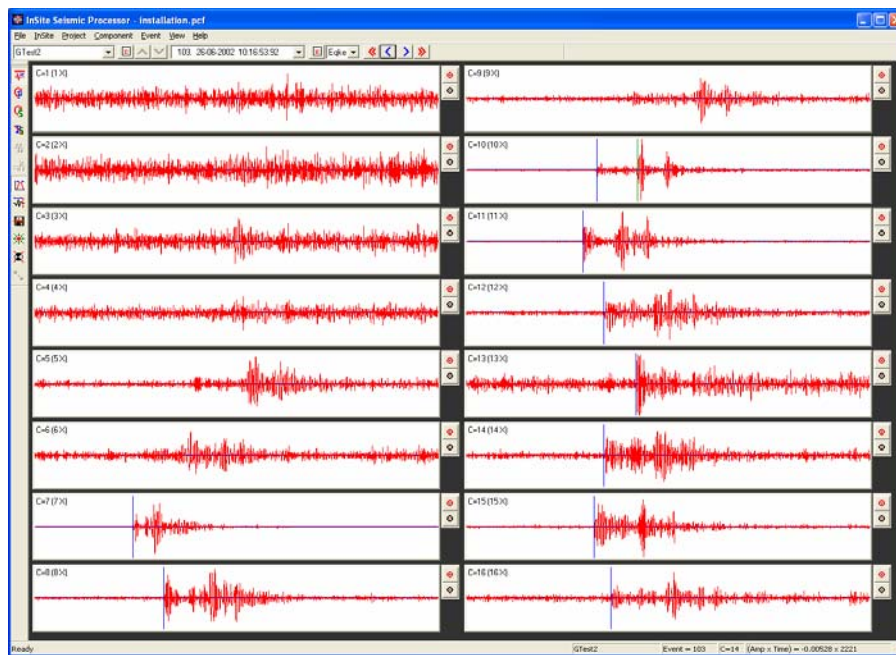

Figure 6-6: *Example waveforms from each of the 16 receiving channels for a 'pencil-lead break' test undertaken against the Deposition Hole (DA3545G01) wall 6 metres*

Appendix II   Processing Parameters

Ultrasonic survey processing parameters:

PROCCESSING PARAMETERS	Velocity survey processing
EVENT INITIALISATION	
View/process waveforms by	Channel
Channel-view Width-to-height ratio	6
Waveform Response type	Set from sensor
Sampling time	1
Time units	Microseconds
Pre-signal points	200
Spline sampling time	0.2
Waveform To point	1023
P-Time correction	0
S-Time correction	0
Automatically update Channel Settings	NOT SET
Project Files	NULL

AUTO PICKING	
Allow P-wave-autopicking	YES, Use first peak in the auto-pick function
Back-window length	100
Front-window length	35
Picking Threshold	4
Min. Peak-to-Peak amplitude	0
Allow S-Wave Autopicking	YES, Use first peak in the auto-pick function
Back-window length	100
Front-window length	35
Picking Threshold	5
Min. Peak-to-Peak amplitude	0
Allow Automatic Amplitude Picking	YES
Use Velocity Window Picking	YES
P-wave Min. Velocity/Max. Velocity	4500, 6500
S-wave Min. Velocity/Max. Velocity	2500, 3500

CROSS-CORRELATION	
CCR Events	Referenced to a Survey
Reference Component	20041208005920
Reference Event	NULL
Window construction method	Front to Back
Window comparison method	Fixed to reference picks
Window Parameters	Back-window length = 20
	Front-window length=30
	Rise-time multiplier = NULL
	Power to raise waveform =1
	Split to a Spline function = YES
	Obtain absolute waveform= NOT SET

LOCATER	*(not used in velocity surveys)*
Method	SIMPLEX INTO GEIGER
Method settings	Tolerance = 0.01
Simplex settings	LPNorm = 1
	P-wave weighting = 1
	S-wave weighting = 1
	Use Outlier Identification = NOT SET
	Arrival error factor = ×2
Geiger settings	Tolerance (Loc. units) = 0.01
	Step size (Loc.units) = 0.1
	Max. Iterations = 100
	Conditional No. Limit = 10000000000
Velocity Structure	Homogeneous Isotropic
Velocity Structure settings	P-wave velocity = 5973.85 m.s^{-1}
	S-wave velocity = 3342.705 m.s^{-1}
	Attenuation = 200
	Q(S) value = 100
Data to use	P-wave Arrivals Only
Distance units	Metres
Working time units	Microseconds
Min P-wave arrivals	0
Min S-wave arrivals	0
Min Independent arrivals	5
Max. Residual	20
Start point	Start at the centroid of the array
Write report to RPT	NOT SET
Source parameters	Set to calculate automatically

AE processing parameters:

PROCCESSING PARAMETERS   **AE processing**

EVENT INITIALISATION	
View/process waveforms by	Channel
Channel-view Width-to-height ratio	6
Waveform Response type	Set from sensor
Sampling time	1
Time units	Microseconds
Pre-signal points	200
Spline sampling time	0.2
Waveform To point	1023
P-Time correction	0
S-Time correction	0
Automatically update Channel Settings	SET
Project Files	NULL

AUTO PICKING	
Allow P-wave-autopicking	YES, Use max peak in the auto-pick function
Back-window length	100
Front-window length	35
Picking Threshold	5
Min. Peak-to-Peak amplitude	0
Allow S-Wave Autopicking	YES, Use max peak in the auto-pick function
Back-window length	100
Front-window length	35
Picking Threshold	5
Min. Peak-to-Peak amplitude	0
Allow Automatic Amplitude Picking	NOT SET
Use Velocity Window Picking	YES
P-wave Min. Velocity/Max. Velocity	4500, 6500
S-wave Min. Velocity/Max. Velocity	2500, 3500

CROSS-CORRELATION	*(not used in AE processing)*
CCR Events	NOT SET
Reference Component	NOT SET
Reference Event	NULL (not activated)
Window construction method	Individual
Window comparison method	Fixed to reference picks
Window Parameters	Back-window length = 31
	Front-window length = 31
	Rise-time multiplier = NULL
	Power to raise waveform =1
	Split to a Spline function = NOT SET
	Obtain absolute waveform= NOT SET

LOCATER	
Method	SIMPLEX INTO GEIGER
Method settings	Tolerance = 0.01
Simplex settings	LPNorm = 1
	P-wave weighting = 1
	S-wave weighting = 1
	Use Outlier Identification = NOT SET
	Arrival error factor = ×2
Geiger settings	Tolerance (Loc. units) = 0.01
	Step size (Loc.units) = 0.1
	Max. Iterations = 100
	Conditional No. Limit = 10000000000
Velocity Structure	Homogeneous Isotropic
Velocity Structure settings	P-wave velocity = 5985 m.s^{-1}
	S-wave velocity = 3343 m.s^{-1}
	Attenuation = 200
	Q(S) value = 100
Data to use	P-wave Arrivals Only
Distance units	Metres
Working time units	Microseconds
Min P-wave arrivals	0
Min S-wave arrivals	0
Min Independent arrivals	5
Max. Residual	20
Start point	Start at the centroid of the array
Write report to RPT	NOT SET
Source parameters	Set to calculate automatically

EVENT FILTER	
Date and Time	NOT SET
Location volume	Minimum = (235, 880, 420)
	Maximum = (300, 964, 463)
L. Magnitude	NOT SET
Location Error	1
Independent Instruments	Minimum = 0

SOURCE PARAMETERS	
Automatic source-parameter windows	P-wave back window = 10
	P-wave front window = 50
	S-wave back window = 10
	S-wave front window = 50
Source parameter calculations	Min number to use = 3
Automatic source-parameter windows	Apply Q correction = SET
	Source density = 2640
	Source shear modulus = 39131400000
	Av. radiation coefficient: Fp = 0.52 ,Fs = 0.63
Source parameter calculations	Source coefficient: kp = 2.01 , ks = 1.32
Magnitude calculations	Instrument magnitude = 1 * log (ppV) +0
	Moment magnitude = 0.666667 * log(Mo) + -6